DOI: 10.1002/chem.200500400

Guest-Induced Supramolecular Isomerism in Inclusion Complexes of T-Shaped Host 4,4-Bis(4′-hydroxyphenyl)cyclohexanone

Srinivasulu Aitipamula and Ashwini Nangia*[a]

Abstract: The T-shaped host molecule 4,4-bis(4′-hydroxyphenyl)cyclohexanone (**1**) has an equatorial phenol group and a cyclohexanone group along the arms and an axial phenol ring as the stem. The equatorial phenyl ring adopts a "shut" or "open" conformation, like a windowpane, depending on the size of the guest (phenol or *o*/*m*-cresol), for the rectangular voids of the hydrogen-bonded ladder host framework. The adaptable cavity of host **1** expands to 11×15–18 Å through the inclusion of water with the larger cresol and halophenol guests (*o*-cresol, *m*-cresol, *o*-chlorophenol, and *m*-bromophenol) compared with a size of 10×13 Å for phenol and aniline inclusion. The ladder host framework of **1** is chiral ($P2_1$) with phenol, whereas the inclusion of isosteric *o*- and *m*-fluorophenol results in a novel polar brick-wall assembly (7×11 Å voids) as a result of auxiliary C−H···F interactions. The conformational flexibility of strong O−H···O hydrogen-bonding groups (host **1**, phenol guest), the role of guest size (phenol versus cresol), and weak but specific intermolecular interactions (herringbone T-motif, C−H···F interactions) drive the crystallization of T-host **1** towards 1D ladder and 2D brick-wall structures, that is, supramolecular isomerism. Host **1** exhibits selectivity for the inclusion of aniline in preference to phenol as confirmed by X-ray diffraction, ^{1}H NMR spectroscopy, and thermogravimetry-infrared (TG-IR) analysis. The T_{onset} value (140 °C) of aniline in the TGA is higher than those of phenol and the higher-boiling cresol guests (T_{onset} = 90–110 °C) because the former structure has more O−H···N/N−H···O hydrogen bonds than the clathrate of **1** with phenol which has O−H···O hydrogen bonds. Guest-binding selectivity for same-sized phenol/aniline molecules as a result of differences in hydrogen-bonding motifs is a notable property of host **1**. Host–guest clathrates of **1** provide an example of spontaneous chirality evolution during crystallization and a two-in-one host–guest crystal (phenol and aniline), and show how weak C−H···F interactions (*o*- and *m*-fluorophenol) can change the molecular arrangement in strongly hydrogen-bonded crystal structures.

Keywords: crystal engineering · host–guest systems · hydrogen bonds · inclusion compounds · supramolecular chemistry

Introduction

Host–guest inclusion compounds make a significant contribution to the growing field of crystal engineering and supramolecular chemistry because they are important for both fundamental and utilitarian reasons.[1] These hollow, porous solids have applications in tailored catalysts, magnetism, electro-optical and nonlinear optical materials, chemical separation, gas-storage devices, and targeted drug delivery. They also serve as models to better understand complex phenomenon such as chirality evolution, nucleation, crystallization, and ligand–receptor binding. Host frameworks assembled from trigonal[2] and tetrahedral[3] scaffolds include neutral molecules and charged counterions as guests in the void space. Suitably functionalized organic molecules with directed hydrogen-bonding groups have been shown to organize as ladder,[4,5] brick-wall, and parquet-grid[6,7] networks. Despite the significant advances in crystal engineering over the last decade,[8] the rational construction of novel open-framework organic solids is still a continuing challenge. Host frameworks respond to structural changes induced by the guest because of shape/size effects and hydrogen-bonding interactions.[9] Polymorphism in clathrates is another complication.[10] It is not possible to predict the crystal structure[11] of host–guest compounds by computa-

[a] S. Aitipamula, Prof. A. Nangia
School of Chemistry, University of Hyderabad
Hyderabad 500 046 (India)
Fax: (+91) 40-2301-1338
E-mail: ashwini_nangia@rediffmail.com

Supporting information for this article (proton NMR spectrum and thermal ellipsoid plots of the two-in-one crystal **1**·phenol·aniline (2:1:1) and FTIR spectra of vapor evolved from **1**·aniline) is available on the WWW under http://www.chemeurj.org/ or from the author.

tional methods because they have multiple components in the unit cell, the molecules are typically of a large size, and they have several conformational degrees of freedom. For these reasons, even though one may design a host molecule through retrosynthetic design[8a] or structural database analysis,[8c] the only way to develop a new open-framework building-block is by carrying out inclusion experiments. To this end, two broad approaches are being pursued. Metal–ligand coordination bonding is extensively used in the modular assembly of extended porous solids and low-density frameworks.[12] The inclusion of gases and volatile liquids in a van der Waals confinement and separation of enantiomers through hydrogen-bond-mediated self-assembly is another contemporary topic.[13] An advantage of the self-assembly approach to host–guest structures[1g] is that inclusion of the guest takes place in a milder process, usually under ambient temperature and pressure, than the high pressure required to force the guest into the zeolite cage.

The construction of ladder, brick-wall, parquet-grid, and bilayer networks with large cavities using metal centers at the T-node in *exo*-functional ligands with square-planar, octahedral, or trigonal-bipyramidal geometry, notably 4,4′-bipyridine and its homologues, has been well studied in coordination polymers.[8b] On the other hand, fewer ladder, brick-wall, and parquet-grid structures have been built from T-shaped organic molecules because standard bond angles at the carbon atom are 120° (trigonal), 109° (tetrahedral), and 180° (linear). The known examples of organic networks built from T-shaped molecules[4,6] are generally devoid of cavities and channels for the enclathration of small molecules. MacGillivray and Coppens and their co-workers[7] reported the first example of a T-shaped organic supermolecule to exhibit guest-induced supramolecular isomerism: the O–H···N hydrogen-bonded adduct of *C*-methylcalix[4]resorcinarene in a flat cone conformation with a 4,4′-bipyridine spacer function as the supramolecular T-node (Figure 1a) in a host brick-wall sheet. We recently showed that the H-shaped tetraphenol molecule, 1,4-bis[bis(4′-hydroxyphenyl)-methyl]benzene[14] (Figure 1b), forms ladder hydrogen-bonded networks with CH_3CN/dioxane guests and hexagonal cavities in EtOH/MeOH clathrates. The architectural isomerism of a host framework driven by guest-template[1d] or host tuning[2e] continues to interest crystal engineers in their search for soft and adaptable organic inclusion compounds.

The T-shaped molecule 4,4-bis(4′-hydroxyphenyl)cyclohexanone (**1**) forms a self-inclusion channel structure in the solid state (guest-free form) with one symmetry-independent molecule viewed as the host and the other as the guest (Figure 1c, d).[15] Encouraged by this preliminary result, we now report the inclusion adducts of **1** with some phenolic guests (Figure 1e). Host **1** assembles as hydrogen-bonded ladders with phenol, *o*-cresol, *m*-cresol, *o*-chlorophenol, and *m*-bromophenol guests. The host cavity can adapt to guest size and expands through the inclusion of water with the larger cresol and halophenol guests. Supramolecular isomerism to a novel type of "polar" brick-wall assembly is observed in *o*- and *m*-fluorophenol clathrates of the T-shaped host **1**. Interestingly, this host molecule forms isostructural inclusion adducts with phenol and aniline separately as well as a two-in-one guest–host crystal (space group $P2_1$) and exhibits good selectivity for the inclusion of aniline in preference to phenol.

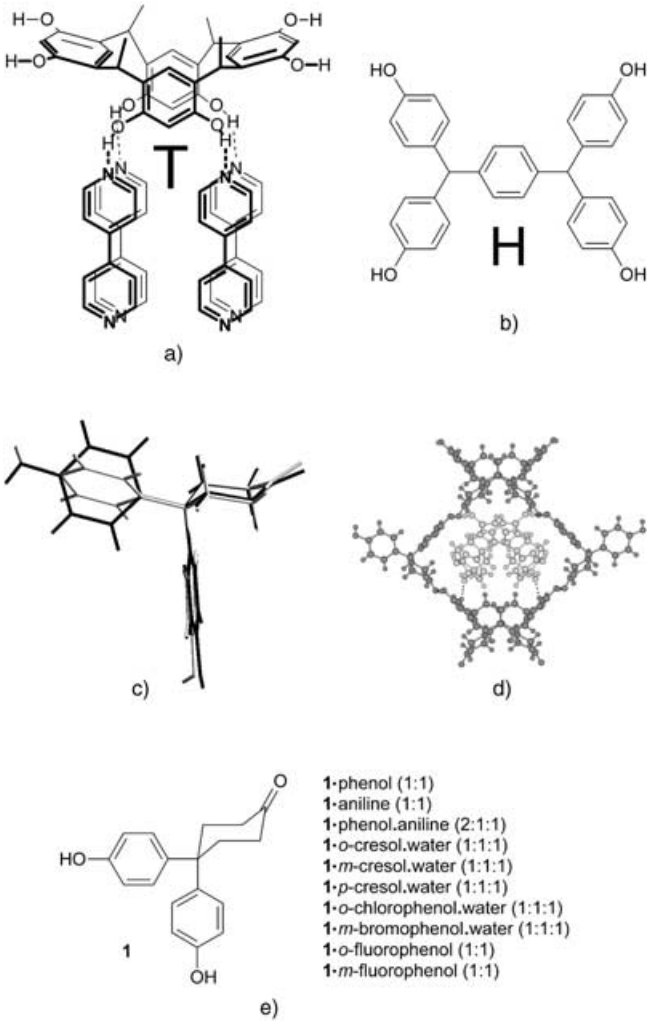

Figure 1. a) T-shaped host supermolecule[7] and b) H-shaped host.[14] c) Overlay of two conformations of the T-shaped host molecule **1** and d) its self-host–guest channel inclusion structure.[15] e) Host–guest structures of **1** discussed in this paper.

Results and Discussion

It was planned to design the title host **1** through functional-group modification of 1,1-bis(4′-hydroxyphenyl)cyclohexane (**2**). Toda and Nassimbeni[16] have reported several host–guest structures of **2** with cresols[16b] and picolines,[16e] and the selective enclathration of *p*-phenylenediamine and *p*-phenylenediol over their *o*-isomers;[16d,f] s-*trans* and s-*cis* conformers of the β-ionone[16c] diene fragment have been isolated in the host lattice of **2**. We have noted that O–

H···O hydrogen-bond chains of **2** with phenol and alcohol-type guests[16b,g] are infinite but the motifs are finite (2–3 hydrogen bonds) with C=O functionalized guests[16a,h] (Scheme 1). The cyclohexane rings of neighboring host molecules **2** close-pack through nonspecific and weak van der Waals (hydrophobic) interactions because they do not have hydrogen-bonding donor/acceptor groups. We reasoned that the supramolecular behavior of **2** could be modified by introducing a strong acceptor group, for example, a ketone, so that specific and directional O–H···O hydrogen bonds extend the host structure into regular cavities and channels because of the C=O stopper group.

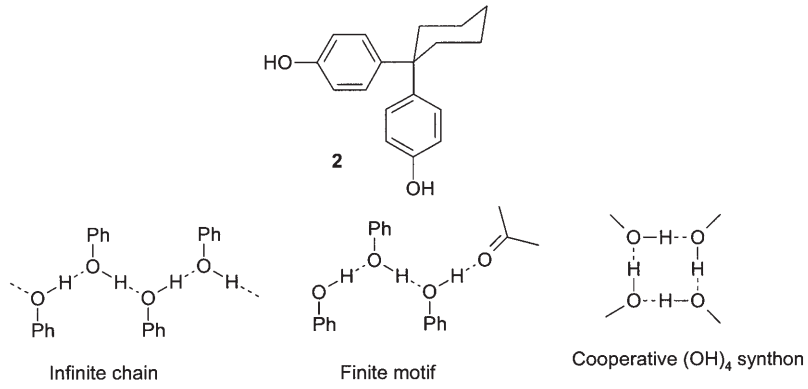

Scheme 1. O–H···O synthons in clathrates of **1** and **2**.

Bis(4-hydroxyphenyl)cyclohexanone (**1**) was readily prepared by the acid-catalyzed condensation of cyclohexane-1,4-dione with two equivalents of phenol.[17] Host **1** was crystallized from several phenolic solvents to obtain single crystals for X-ray diffraction analysis. DSC and TGA confirmed the phase purity, guest stoichiometry, and release of volatile vapors from the host lattice. Competition experiments on the selective inclusion of aniline compared to phenol were monitored by ^{1}H NMR spectroscopy and by analyzing the infrared spectrum of the vapor evolved in thermogravimetry (TG-IR). Crystal-lattice energy calculations validate the promiscuous inclusion behavior of host **1** and hydrogen-bond energies explain the tight binding of aniline relative to the similar-sized phenol guest. In its clathrates, the equatorial phenyl ring in the T-shaped molecule **1** can adopt two different low-energy conformations, referred to as the "open" and "shut" windowpanes of the host cavity, which can tune the void dimensions depending on the guest size.

Molecular ladder inclusion structures

1·phenol (1:1): Crystallization of **1** from phenol afforded single crystals of a 1:1 adduct in the $P2_1$ chiral space group (Table 1) with two molecules of **1** (A and B) and two phenol molecules (C and D) in the asymmetric unit. The cyclohexanone rings of the A and B molecules adopt the stable chair conformation. The conformations of the symmetry-independent host molecules are identical except for the orientation of the hydroxy group in the axial phenol ring (Figure 2a). The axial and equatorial phenol rings are roughly orthogonal to the mean plane of the cyclohexanone ring, making angles of 85.0, 89.8 and 87.5, 88.7° with the A and B molecules, respectively. Four symmetry-independent host and guest molecules aggregate through O–H···O hydrogen bonds (1.84 Å, 165.4°; 1.71 Å, 167.5°; 1.74 Å, 170.2°; Table 2) to generate rectangular voids of 10×13 Å for guest inclusion (Figure 3a). Phenol guests (C and D) are hydrogen-bonded to molecular ladders of A and B host molecules through O–H···O interactions (1.78 Å, 164.5°; 1.73 Å, 177.8°; 1.80 Å, 170.2°), and such ladders extend to form layers in the *ab* plane that stack down the *c* axis with an offset of half the ladder rung of the hydrogen-bonded ladders (see Figure 9a). All the hydroxy hydrogen atoms are involved in O–H···O hydrogen bonds, acting both as donors and acceptors, except for the hydroxy groups of the B host equatorial phenol and the D guest molecule, which donate a hydrogen atom only. In contrast to the infinite chain of O–H···O bonds in **2**·phenol,[16b] the motif is truncated to 2–4 O–H···O hydrogen bonds by the C=O acceptor in **1**·phenol. Such a change in the hydrogen bonding for host **1** was expected because of the carbonyl cap (Scheme 1).

1·aniline (1:1): The aniline solvate of **1** is isostructural to its phenol complex ($P2_1$). There are two molecules each of **1** and aniline in the asymmetric unit. One of the aniline molecules (D) is orientationally disordered with a site occupancy factor (s.o.f.) of 77:23 such that it mimics *o*-phenylenediamine. The conformation of the host molecules (Table 3) and the hydrogen-bond network is virtually identical in both complexes but guest molecules are organized slightly differently (Figure 2b and Figure 3b). Guest molecules are bonded to the host lattice by tetrahedral hydrogen-bond coordination around the amine nitrogen atom (N–H···O and O–H···N, Table 2) and an N–H···N interaction connects the aniline guest molecules. Whereas the hydrogen-bond chains are finite in **1**·phenol, the guest and host molecules in **1**·aniline form an infinite cooperative array of O–H···O, N–H···O, and O–H···N hydrogen bonds because the guest molecule has two NH donors.

1·phenol·aniline (2:1:1): Two structural features of **1**·phenol and **1**·aniline are noteworthy for planning the next experiment. 1) Their host–guest adducts are isostructural.[1f] 2) Host···guest hydrogen-bonding along the unique *b* axis is identical (Figure 4). Based on these observations, we attempted the inclusion of both phenol and aniline guests in the ladder network of host **1**. After several phenol/aniline

Table 1. Crystallographic data for the inclusion complexes of host **1**.

Compound	**1**·phenol	**1**·aniline	**1**·phenol·aniline	**1**·*o*-cresol	**1**·*m*-cresol
empirical formula	$(C_{18}H_{18}O_3)_2{\cdot}(C_6H_6O)_2$	$(C_{18}H_{18}O_3)_2{\cdot}(C_6H_7N)_2$	$(C_{18}H_{18}O_3)_2{\cdot}C_6H_7N{\cdot}C_6H_6O$	$C_{18}H_{18}O_3{\cdot}C_7H_8O{\cdot}H_2O$	$C_{18}H_{18}O_3{\cdot}C_7H_8O{\cdot}H_2O$
formula wt.	752.86	750.20	750.67	408.47	408.47
crystal system	monoclinic	monoclinic	monoclinic	triclinic	triclinic
space group	$P2_1$	$P2_1$	$P2_1$	$P\bar{1}$	$P\bar{1}$
T [K]	100	100	298	298	298
a [Å]	9.767(2)	9.782(2)	9.8789(7)	10.143(2)	9.754(2)
b [Å]	19.669(4)	19.906(4)	19.7801(14)	11.208(2)	11.306(2)
c [Å]	9.937(2)	9.932(2)	10.0768(7)	11.848(2)	11.516(2)
α [°]	90.00	90.00	90.00	62.37(3)	108.77(3)
β [°]	91.29(3)	90.98(3)	91.2470(10)	70.39(3)	108.68(3)
γ [°]	90.00	90.00	90.00	65.38(3)	99.61(3)
Z	2	2	2	2	2
V [Å^3]	1908.3(7)	1933.6(7)	1968.6(2)	1067.7(4)	1086.3(4)
λ [Å]	0.71073	0.71073	0.71073	0.71073	0.71073
ρ_{calcd} [g cm^{-3}]	1.310	1.290	1.321	1.271	1.249
F [000]	800	800	832	436	436
μ [mm^{-1}]	0.088	0.085	0.090	0.088	0.086
θ [°]	3.56–29.34	3.55–27.50	2.06–26.04	1.97–27.50	1.99–27.47
index ranges	$-13 \le h \le 13$	$-12 \le h \le 12$	$-12 \le h \le 12$	$0 \le h \le 13$	$0 \le h \le 12$
	$-11 \le k \le 26$	$-25 \le k \le 25$	$-22 \le k \le 24$	$-12 \le k \le 14$	$-14 \le k \le 14$
	$-13 \le l \le 13$	$-7 \le l \le 12$	$-12 \le l \le 12$	$-14 \le l \le 15$	$-14 \le l \le 14$
reflections collected	12609	12429	10936	4860	5256
unique reflections	5414	8478	4004	4860	4962
observed reflections	4992	6469	3302	3250	3145
R_1 [$F_o > 4\sigma(F_o)$]	0.0379	0.0600	0.0437	0.0465	0.0561
wR_2	0.0872	0.1465	0.1103	0.1369	0.1886
goodness-of-fit	1.070	1.054	1.039	1.072	1.018

Compound	**1**·*p*-cresol	**1**·*o*-chlorophenol	**1**·*m*-bromophenol	**1**·*o*-fluorophenol	**1**·*m*-fluorophenol
empirical formula	$C_{18}H_{18}O_3{\cdot}C_7H_8O{\cdot}H_2O$	$C_{18}H_{18}O_3{\cdot}C_6H_5ClO{\cdot}H_2O$	$C_{18}H_{18}O_3{\cdot}C_6H_5BrO{\cdot}H_2O$	$C_{18}H_{18}O_3{\cdot}C_6H_5FO$	$C_{18}H_{18}O_3{\cdot}C_6H_5FO$
formula wt.	408.47	428.89	473.35	394.42	394.42
crystal system	monoclinic	triclinic	triclinic	triclinic	triclinic
space group	$P2_1/c$	$P\bar{1}$	$P\bar{1}$	$P\bar{1}$	$P\bar{1}$
T [K]	100	100	100	100	100
a [Å]	9.8613(5)	9.8383(19)	9.7051(8)	9.6615(8)	9.6049(7)
b [Å]	18.6196(9)	11.101(2)	11.2980(10)	10.8699(9)	10.7071(8)
c [Å]	12.2058(6)	11.707(2)	11.7938(10)	11.0142(10)	10.9583(8)
α [°]	90.00	62.614(2)	114.5020(10)	61.4910(10)	61.9410(10)
β [°]	107.3830(10)	70.481(2)	106.9160(10)	83.069(2)	78.9950(10)
γ [°]	90.00	66.716(2)	99.0690(10)	77.2450(10)	85.1290(10)
Z	4	2	2	2	2
V [Å^3]	2138.79(18)	1024.5(3)	1066.73(16)	991.21(15)	976.20(12)
λ [Å]	0.71073	0.71073	0.71073	0.71073	0.71073
ρ_{calcd} [g cm^{-3}]	1.269	1.390	1.474	1.322	1.342
F [000]	872	452	488	416	416
μ [mm^{-1}]	0.087	0.221	1.960	0.095	0.097
θ [°]	2.06–26.01	1.99–25.69	2.07–26.04	2.10–26.37	2.14–26.05
index ranges	$-10 \le h \le 11$	$-11 \le h \le 11$	$-11 \le h \le 11$	$-11 \le h \le 11$	$-11 \le h \le 11$
	$-14 \le k \le 22$	$-10 \le k \le 13$	$-13 \le k \le 13$	$-13 \le k \le 13$	$-13 \le k \le 13$
	$-15 \le l \le 14$	$-14 \le l \le 14$	$-14 \le l \le 14$	$-12 \le l \le 13$	$-13 \le l \le 13$
reflections collected	10503	9262	12965	7617	16259
unique reflections	3991	3848	4181	4028	3841
observed reflections	3381	2546	3911	3464	3530
R_1 [$F_o > 4\sigma(F_o)$]	0.0390	0.0546	0.0242	0.0511	0.0369
wR_2	0.0955	0.1313	0.0640	0.1326	0.0938
goodness-of-fit	1.034	1.028	1.100	1.050	1.055

ratios were tried, single crystals were obtained from a crystallization batch containing phenol/aniline 10:1. Details of mixed-solvent experiments are discussed later in the section on the selective inclusion of aniline. ^{1}H NMR spectra showed the presence of both aniline and phenol (see the Supporting Information) and X-ray diffraction analysis solved the structure in the $P2_1$ space group with similar cell values to those of the pure host–guest structures (Table 1). The crystal structure of $(\mathbf{1})_2$·phenol·aniline shows the inclusion of both aniline and phenol in the rectangular voids of an isostructural host lattice (Figure 3c). Whereas aniline molecules are fully ordered, the phenol guests are disor-

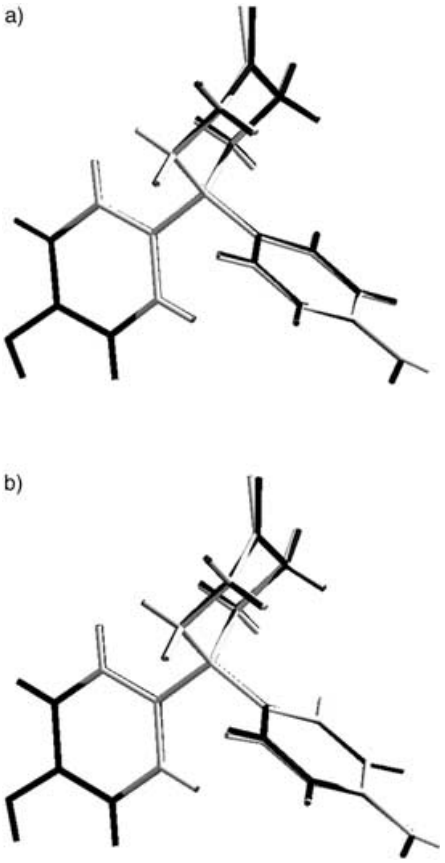

Figure 2. Overlay of symmetry-independent host molecules A and B (shaded differently) in inclusion crystals of a) phenol and b) aniline. The conformations are identical except for the orientation of the axial phenol hydroxy group. See Table 3 for ring interplanar angles in **1**.

dered with 0.79 and 0.21 site occupancy. The aniline guests are hydrogen-bonded to one side of the molecular ladder whilst the phenol molecules are bonded to the other side. There is no phenol···aniline hydrogen-bonding. The inclusion of both phenol and aniline as guests is remarkable because strong, saturated hydrogen bonds form between their complementary functional groups.[18] We were able to locate both the amino and the major occupancy hydroxy hydrogen atoms in the difference electron-density map. Since oxygen and nitrogen atoms are about the same size (they differ by one electron for X-radiation), the molecular constituents of the binary guest·host structure **1** were further confirmed by replacing the guest nitrogen and oxygen atoms in structure refinement cycles by oxygen and nitrogen, respectively. The incorrectly assigned structures show enlarged thermal ellipsoids when nitrogen is replaced with oxygen, and shrunk ellipsoids when oxygen is replaced with nitrogen;[19] the residual *R* factor is higher for incorrectly assigned guest atoms (see the Supporting Information). This means that the location of aniline and phenol in the three-component host–guest structure, as determined by X-ray diffraction (Table 1), is correct. To our knowledge, this is a rare example of two guest molecules, which otherwise form strong hydrogen bonds, being separated from each other in the constrained microenvironment of the host lattice. This two-guest clathrate was designed by using structural mimicry of the 1D hydrogen-bond chains shown in Figure 4. We have

Table 2. Hydrogen bond distances in clathrates of **1** (neutron normalized).

Compound	D−H···A	H···A [Å]	D···A [Å]	D−H···A [°]
1·phenol	O2−H2A···O1	1.74	2.718(2)	170.2
	O3−H3A···O2A	1.84	2.808(2)	165.4
	O4−H4A···O2	1.80	2.775(2)	170.2
	O4A−H4AA···O3A	1.73	2.710(2)	177.8
	O3A−H3AA···O1A	1.71	2.682(2)	167.5
	O2A−H2AA···O4A	1.78	2.736(2)	164.5
1·aniline	O2−H11···N1	1.79	2.734(4)	160.3
	O3−H12···O1	1.73	2.706(3)	171.7
	O2A−H21···O1A	1.82	2.773(3)	162.3
	O3A−H22···O2	1.78	2.736(3)	163.0
	N1−H31···N1B	2.14	3.133(4)	168.5
	N1−H32···O3	2.08	2.990(4)	149.5
	N1B−H41A···O3A	2.03	3.009(4)	163.0
	N1B−H42A···O1A	2.01	3.013(4)	170.5
1·phenol·aniline	O5−H1···O6	1.82	2.784(5)	164.5
	O4−H2···O2	1.86	2.817(6)	162.3
	O2−H2A···N1	1.82	2.774(6)	163.6
	O1−H4···O3	1.77	2.729(5)	165.2
	O7−H7A···O5	1.89	2.869(7)	175.3
	N1−H7B···O1	1.87	2.858(6)	165.6
1·*o*-cresol	O4−H1···O5	1.71	2.674(3)	165.0
	O5−H5BB···O4	1.91	2.822(3)	152.8
	O3−H2···O1	1.80	2.776(2)	170.9
	O5−H5AA···O2	1.89	2.845(2)	162.8
	O2−H3···O1	2.08	3.033(3)	162.8
1·*m*-cresol	O1−H1···O2	1.87	2.849(4)	175.5
	O5−H5AA···O4	1.77	2.715(3)	160.9
	O2−H2AA···O3	1.92	2.832(3)	152.4
	O2−H2AB···O5	1.86	2.817(4)	164.5
	O3−H3A···O2	1.79	2.734(3)	159.1
1·*p*-cresol	O5−H5A···O1	1.83	2.743(2)	152.7
	O5−H5B···O2	1.76	2.733(2)	171.3
	O4−H2···O5	1.81	2.789(2)	172.7
	O2−H5···O3	1.74	2.716(2)	174.0
	O1−H6···O5	1.72	2.692(2)	168.0
1·*o*-chlorophenol	O4−H28···O5	1.95	2.907(4)	164.8
	O1−H25···O4	1.83	2.795(4)	166.1
	O2−H26···O1	1.64	2.615(4)	169.3
	O1−H27···O2	1.98	2.840(4)	145.1
	O3−H29···O5	1.79	2.765(3)	172.2
1·*m*-bromophenol	O5−H25···O1	1.69	2.663(2)	170.9
	O2−H26···O4	1.73	2.688(2)	164.0
	O4−H28···O2	1.82	2.744(2)	155.3
	O3−H29···O4	1.82	2.801(2)	174.2
	C7−H7···O3	2.36	3.426(2)	168.1
	O4−H27···O5	1.77	2.728(2)	162.3
1·*o*-fluorophenol	O4−H4A···F1	2.15	2.757(3)	118.3
	O4−H4A···O3	1.95	2.832(2)	147.4
	O2−H18···O1	1.69	2.625(2)	157.9
	O3−H19···O2	1.77	2.748(2)	177.0
1·*m*-fluorophenol	O2−H2···O1	1.71	2.619(2)	151.7
	O3−H3···O2	1.78	2.762(1)	174.7
	O4−H4A···O3	1.78	2.742(2)	166.6

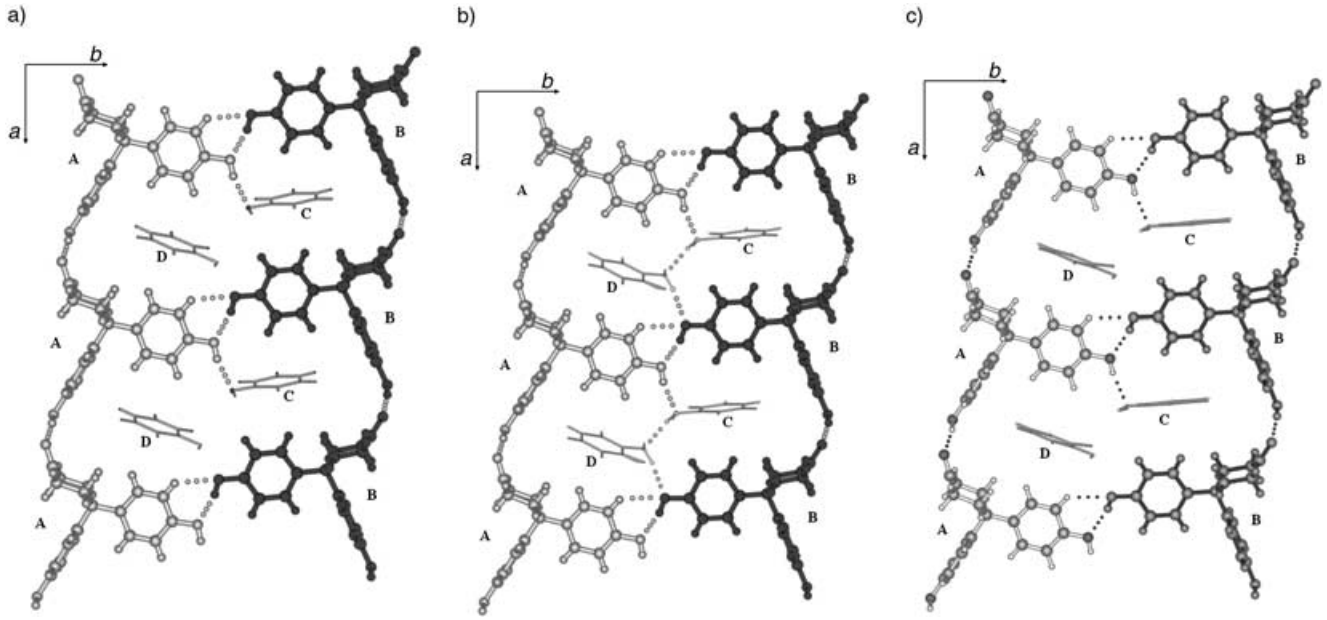

Figure 3. Chiral ladder hydrogen-bond network of T-shaped host molecule **1**. Inclusion of a) phenol and b) aniline guests in cavities of 10×13 Å. The phenol (D) molecules are hydrogen-bonded to the next layer (not shown) and the aniline (D) guest is disordered (s.o.f. 0.77:0.23). c) Inclusion of both aniline (C) and phenol (D) molecules in an isostructural host ladder. Aniline molecules are located on the right hand side of the chiral ladder and phenol molecules on the left. Disordered phenol (D) molecules (s.o.f. 0.79:0.21) hydrogen bond to the next layer (not shown). Host molecules (A, B) are shown as ball and stick models and guest molecules (C, D) in a wire frame.

Table 3. Conformation of T-host **1** in clathrates, tabulated as the angle between the mean plane of the cyclohexanone ring and the equatorial and axial phenol ring planes.

Guest	Equatorial phenol [°]	Axial phenol [°]	Host Ph conformation	Void size [Å]	Volume occupied by guest [%][a]	Packing fraction [%][a]
none	A 85.9	A 88.4	–	–	–	70.1
	B 38.8	B 86.1				
phenol	A 89.8	A 85.0	shut	10×13	19.8	70.9
	B 88.7	B 87.5				
aniline	A 89.1	A 85.0	shut	10×13	21.0	71.7
	B 89.8	B 86.9				
phenol &	A 89.8	A 84.0	shut	10×13	16.6	70.1
aniline	B 88.7	B 86.4				
o-cresol	16.6	87.6	open	11×18	24.0	69.7
m-cresol	9.0	86.9	open	11×15	22.0	69.0
p-cresol	28.9	78.0	open	11×25	21.9	67.7
o-Cl-phenol	14.7	87.1	open	11×18	25.8	74.2
m-Br-phenol	10.0	86.8	open	11×15	25.4	70.6
o-F-phenol	89.6	88.5	shut	7×11	22.2	71.6
m-F-phenol	89.8	87.1	shut	7×11	22.1	73.4

[a] Calculated by using the Platon software package.

recently shown that 1D isostructurality is a sufficient condition to expect solid solution crystals of C6-substituted steroids.[19] There are examples of two or more guests enclathrated in host channels and capsules,[20] but the guest molecules are usually of a different size and shape. The inclusion of phenol and aniline guests in their respective locations in the above two-in-one structure, and not as a solid solution, underscores the fact that small differences in the hydrogen bonding of these similar size/shape guests with an otherwise identical host scaffold play an important role. The isolation of different guests in distinct channels/voids of microporous solids has potential applications in materials science.

Next we will briefly discuss why these structures adopt the chiral $P2_1$ space group. The tricyclic skeletons of the symmetry-independent A and B molecules of host **1** overlay nicely except for the orientation of the axial phenol hydroxy group. This difference in the orientation of one hydrogen atom (Figure 2) makes these molecules crystallographically distinct instead of mirror-image isomers in the same crystal. Crystallization of achiral or racemic molecules in noncentrosymmetric space groups[21] is a little understood phenomenon even though a proper understanding of such events is important in absolute asymmetric synthesis and catalysis and will shed light on the spontaneous evolution of chirality in Nature. Whereas enantiomorphous inclusion is the norm for chiral host molecules (e.g. steroids, peptides, and cyclodextrins), there are few examples of noncentrosymmetric host–guest structures derived from achiral/racemic components, and the reasons for chiral self-assembly are even less well understood.[1b,c] In the present pair of structures, strong hydrogen-bonding phenol hy-

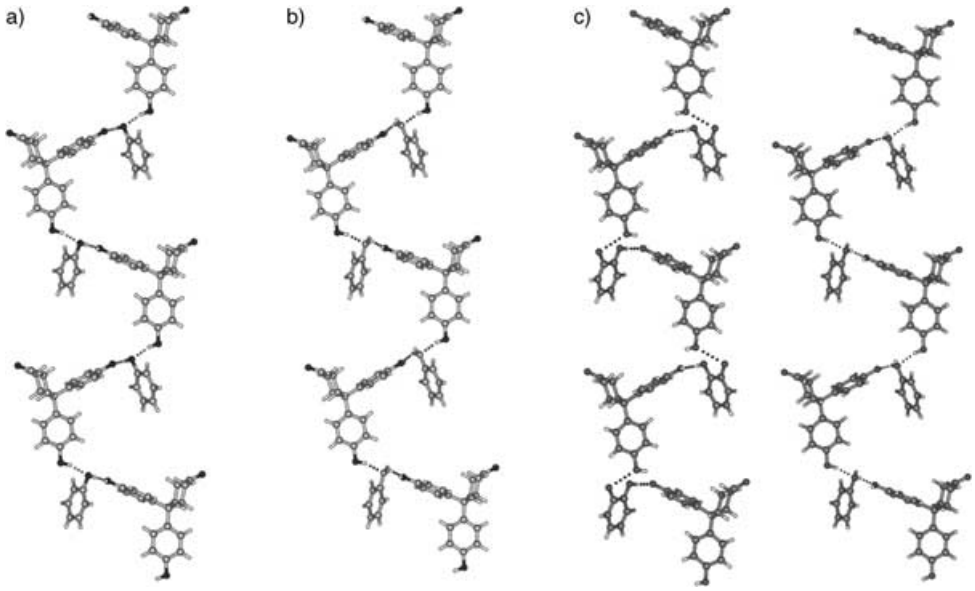

Figure 4. Zigzag chain of screw-axis-related host and guest molecules along the *b* axis in a) **1**·phenol and b) **1**·aniline. c) Host and guest molecules in mixed guest crystal $(\mathbf{1})_2$·phenol·aniline. Note the near identical arrangement of host and guest molecules in pure and mixed guest structures along the unique axis.

droxy groups promote the likelihood of $Z'>1$ and the fact that phenol/alcohol O–H···O hydrogen bonds do not generally aggregate through centrosymmetric motifs, that is, as chains and rings, improves the chances of crystallization in chiral space groups. The probability of crystallization in non-centrosymmetric space groups for monoalcohols (including phenols) (32%) is greater than the global average (20%); the values are 24 and 10% for chiral space groups.[22] Monoamines follow similar statistics. These factors explain the crystallization of phenol/aniline clathrates of **1** in the $P2_1$ space group. Bishop and co-workers[5a] have noted the tendency for racemic diols to crystallize as ladders of (+) or (−) molecules (i.e. as conglomerates) instead of both enantiomers being present in the same hydrogen-bonded ladder.

Cholic acid is the only host molecule for which inclusion adducts with both phenol and aniline have been reported.[23] However, these inclusion crystal structures are not of the same type, with the host molecule adopting an α-*gauche* arrangement with aniline and β-*trans* packing with phenol.[23b] The isostructurality of the phenol and aniline inclusion adducts of **1** could be due to the semi-rigid shape of host **1**, the modular build up of the O–H···O hydrogen-bond network, and the role of guest size in self-assembly. These points are validated by related structures in this paper.

1·*o*-cresol·H_2O (1:1:1) and 1·*o*-chlorophenol·H_2O (1:1:1): Host **1** and *o*-cresol crystallize as a monohydrate in the $P\bar{1}$ space group with one molecule of each component in the asymmetric unit. *o*-Cresol and water form a centrosymmetric O–H···O tetramer synthon (1.71 Å, 165.0°; 1.91 Å, 152.8°), which is linked to the T-shaped molecule **1** through O–H···O hydrogen bonds (1.89 Å, 162.8°). The $(OH)_4$ tetramer synthon (Scheme 1) in this structure is stabilized by the σ-bond cooperativity[24] of the hydroxy donors and acceptors in a cyclic array (homodromic). The centrosymmetric ladder network in the *bc* plane (Figure 5a) has a larger cavity size (11×18 Å) than the phenol and aniline clathrates. O_{water}–H···O_{host} hydrogen bonds serve as bridges between the host ladder network and the guest molecules. The ladders stack in a terraced fashion with an offset of half the ladder rung and height along the *c* and *b* axes (see Figure 9b). Interestingly, the $(OH)_4$ tetramer synthon in hydrates of **1** was also identified in step-ladders of dialcohol structures.[5a]

The crystal structure of **1**·*o*-chlorophenol·H_2O is identical to that of the *o*-cresol adduct (Figure 5b). In this case, methyl/halogen exchange occurs without disturbance of the crystal packing[25] because these groups have a similar size (van der Waals volumes: Me, 24 Å^3; Cl, 20 Å^3).[25c] The axial phenol hydroxy group connects neighboring ladders through O–H···O interactions (*o*-Cl-phenol: 1.95 Å, 164.8°; *o*-cresol 2.08 Å, 162.8°).

1·*m*-cresol·H_2O (1:1:1) and 1·*m*-bromophenol·H_2O (1:1:1): The ladder consists of a $(OH)_4$ synthon between water and the host **1** instead of water and the guest molecules. The perfect ladder network (Figure 5c) has rectangular voids of 11×15 Å in the *bc* plane and such ladders stack with an offset along the *a* axis. The *m*-bromophenol solvate of **1** (bromine volume = 26 Å^3) has an identical arrangement of host molecules (Figure 5d). There is an O_w–H···O_{phenol} hydrogen bond between the (−2 0 1) planes in both structures (1.79 Å, 159.1°; 1.77 Å, 162.3°). Significantly, the orientation of the guest molecules is different. The methyl group of the *m*-cresol guest points towards the host cyclohexanone C=O moiety (Figure 5c), whereas the bromine atom of *m*-bromophenol points in the opposite direction (Figure 5d).

Differences in the orientation of the methyl and bromine guest atoms could be due to two factors. 1) A weak (Me)C–H···π(phenol) interaction[26] is optimized in **1**·*m*-cresol (C–H···π: 3.28 Å, 127.4°), whereas if the bromine atom was to occupy the same position it would be farther away from the surface of the phenyl ring. Additional C–H···O interactions (2.36 Å, 168.1°) between *m*-bromophenol guests bring these guest molecules closer to each other (see Figure 5d), and in effect farther away from the phenol π-cloud centroid. In the inverted orientation observed in the crystal, the bromine atom points towards the midpoint of a C=C bond (3.37 Å, 176.0°) of the phenyl ring, which results in a C–Br···π inter-

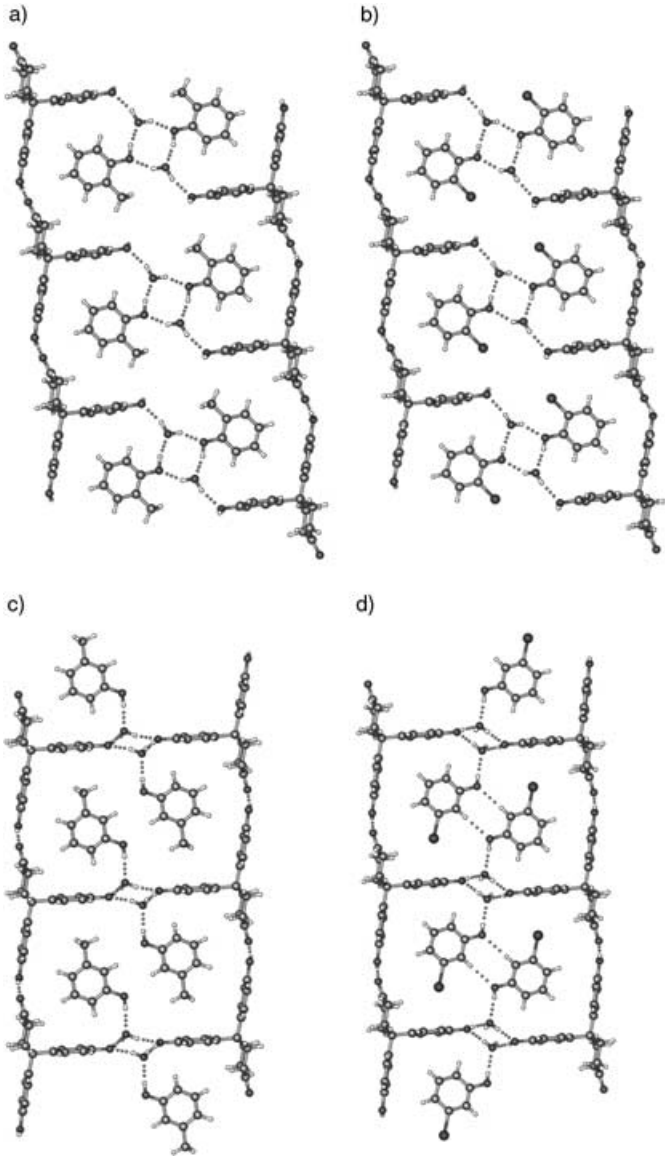

Figure 5. Expanded ladder networks of **1** formed by the inclusion of water in substituted phenols: a) *o*-cresol, b) *o*-chlorophenol, c) *m*-cresol, and d) *m*-bromophenol. Substitution of the phenol guest changes the host–guest ladder structure. Host structures of the *o*-phenols (a, b, void size = 11 × 18 Å) and the *m*-phenols (c, d, void size = 11 × 15 Å) are identical. *o*-Cresol and *o*-Cl-phenol guests are orientated in the same way, but *m*-cresol and *m*-Br-phenol point in opposite directions (see text for explanation). These centrosymmetric structures incorporate the $(OH)_4$ tetramer synthon.

action.[21e] 2) In lattice-energy calculations (see the Experimental Section), the methyl group of the *m*-cresol clathrate was replaced by a bromine atom and vice versa. Minimized lattice energies of the observed crystal structures are lower than those of the putative structures in both cases (*m*-cresol: −95.28 and −91.54 kcal mol^{-1} (observed/putative); *m*-bromophenol: −120.07 and −112.20 kcal mol^{-1} (observed/putative)). Host **1** did not afford single crystals with *m*-Cl-phenol and *o*-Br-phenol guests, thus preventing analysis of the complete series of structures.

The inclusion structures of host **1** with cresols and halophenols are centrosymmetric in contrast to the chiral inclusion crystals obtained with phenol and aniline. This could be because of the bulkier guest molecule and inclusion of water in the crystal. Centrosymmetric packing is favored with cresol-sized guests because of the expanded cavity size, O−H···O tetramer synthon between inversion-related molecules, and the fact that there are no direct phenol···phenol hydrogen bonds; the latter motifs tend to avoid the inversion center.[22] The phenol and *o*/*m*/*p*-cresol inclusion adducts of the Toda–Nassimbeni host **2** are isomorphous and centrosymmetric.[16b] In contrast, host **1** crystallizes in a chiral host–guest structure with phenol but forms centrosymmetric adducts with the cresols. Moreover, the structure of the *p*-cresol guest is quite different (discussed next) to that of the *o*/*m*-cresols. T-shaped keto-diphenol **1** not only adds to the examples of organic ladders built from other building blocks such as dialcohols,[5a] secondary ammonium halides,[5d] and [*n*]-ladderanes,[5f] but it also exhibits guest inclusion in tunable rectangular voids.

Brick-wall host structures

1·*p*-cresol·H_2O (1:1:1): The inclusion of *p*-cresol results in further expansion of the rectangular voids. Now the T-nodes of alternate ladder rungs twist outwards to form a distorted brick-wall network (Figure 6) by bonding with another molecule of **1**. The $(OH)_4$ tetramer between the host and guest molecules is similar to that in the *m*-cresol ladder, but the rotation of the T-node changes the network topology from a 1D ladder to a 2D brick-wall structure. Two *p*-cresol molecules (length 6.5 Å) are unable to fit into the ladder host framework, which has an inter-rung distance of approximately 11 Å, and so alternate host molecules rotate outwards to form large cavities of 11 × 25 Å in an isomeric brick-wall network. Thus, guest size and shape play an important role in guiding the orientation of host phenol rings and in turn the supramolecular architecture. Phenol, *o*-cresol, *m*-cresol, and *p*-cresol cause a graded change in hydrogen bonding, cavity size, and hence in the host–guest framework.

The effect of introducing a strong electronegative atom, like fluorine, in the guest template is discussed next.

1·*o*- and *m*-fluorophenol (1:1): The crystal structure of *o*-fluorophenol and host **1** has linear chains of O−H···O hydrogen bonds (1.77 Å, 177.0°) between the phenol hydroxy groups along the *b* axis. The free hydroxy group of this chain bonds to the C=O group of an adjacent chain (1.69 Å, 157.9°) to form a brick-wall network in the *bc* plane (Figure 7a). Guest molecules located in rectangular voids of 7 × 11 Å are connected to inversion-related brick-wall layers through O−H···O hydrogen bonds (1.95 Å, 147.4°) and the framework adopts the $P\bar{1}$ space group. The *m*-fluorophenol solvate has an identical host framework (Figure 7b) with the minor difference that inversion-related brick-wall networks stack by hydrophobic close-packing.

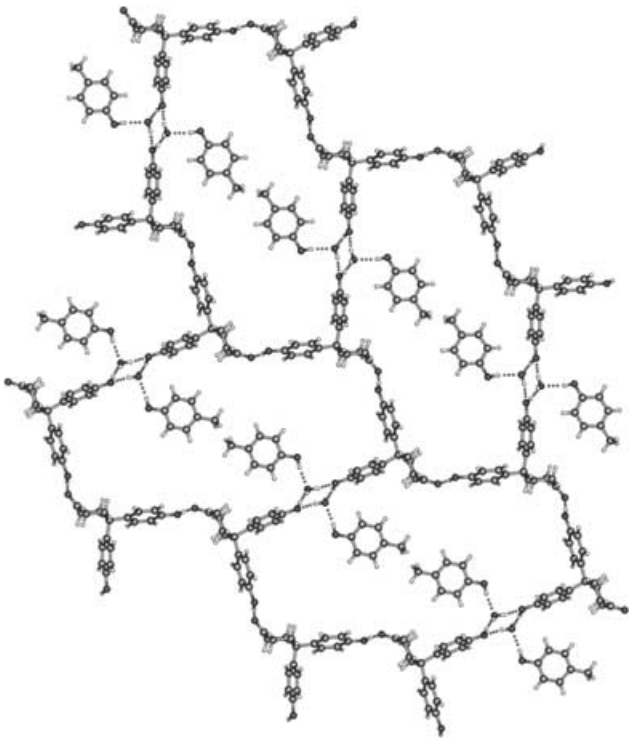

Figure 6. *p*-Cresol inclusion adduct of host **1**. The cavity size expands to 11×25 Å by rotation of the T-shaped host molecule to form a 2D brick-wall network, a supramolecular isomer of the 1D ladder. The distorted brick-wall grid has (6,3) network topology.

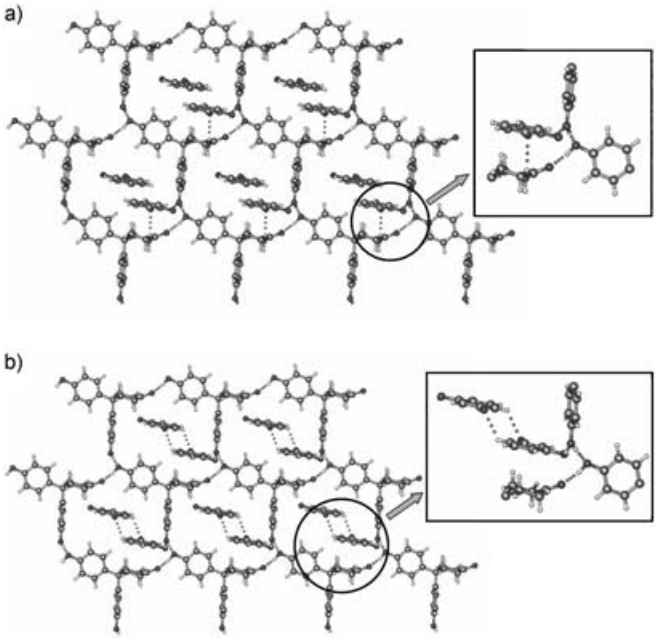

Figure 7. Polar 2D brick-wall layer of host **1** with a) *o*-fluorophenol and b) *m*-fluorophenol guests (7×11 Å voids). Note the alternation of molecular and supramolecular nodes. This is a novel self-assembly mode for the T-shaped molecule. C–H···F interactions are shown in the insert.

Given the importance of guest size in directing the assembly of host **1**, the striking difference between the crystal structures involving the phenol and fluorophenol guests (van der Waals radius: H 1.20 Å; F 1.47 Å) must be rationalized. The high electronegativity of fluorine (F 4.0; H 2.1; C 2.5; Pauling scale) directs antiparallel orientation of the fluorinated guests in the host cavity, which explains the crystallization of the fluorophenol network in the centrosymmetric $P\bar{1}$ space group in contrast to the $P2_1$ space group of the phenol network. There is an intramolecular O–H···F interaction (2.15 Å, 118.3°) and a short C–H···F interaction (2.52 Å)[27] between the activated α-CH moiety of cyclohexanone and the *o*-fluorophenol. *m*-Fluorophenol guests in the channel are connected through a C–H···F dimer interaction of 2.67 Å length (see insert in Figure 7). In related examples, the orientation of *o*- and *p*-fluorophenol molecules in the α-cyclodextrin cavity has been ascribed to O–H···F–C interactions.[28a] Differences in the orientation of fluorobenzene guests in the cavity of *p-tert*-butylcalix[4]arene and guest-induced changes to the host framework have been explained through electrostatic and short-range interactions.[28b] We suggest that guest-induced supramolecular isomerism from the ladder to the brick-wall framework for fluorophenol guests is caused by weak yet structure-interfering C–H···F interactions. It is difficult to properly explain the influence of fluorine substitution on molecular orientation and crystal packing because we still do not know enough about the nature of fluorine interactions.[29] Inclusion experiments with pentafluorophenol and other fluorophenols in host **1** are ongoing to gain a better understanding of this series of structures. Host–guest structures with fluorinated guests could serve as small-molecule models to gain an insight into the binding of fluorinated enzyme inhibitors and drugs to their macromolecular receptors.[30]

Supramolecular networks: Even though V-shaped host molecule **2**[16] is versatile in its inclusion behaviour, it offers structural control of host–guest adducts only along the phenol O–H···O chain motif (infinite or finite). On the other hand, the hydrogen bonds of T-shaped molecule **1** can extend in one or two dimensions to form diverse supramolecular frameworks depending on the guest species (Figure 8). In contrast to the assembly of two host molecules in the ladder and brick-wall networks described so far (Figure 3, Figure 5, and Figure 6), three host molecules are connected through two O–H···O hydrogen bonds at each supramolecular junction in the polar 2D brick-wall structure shown in Figure 7. Whereas the brick-wall network shown in Figure 8c is constructed from molecules at the nodes with hydrogen bonds as the node connectors, the arrangement shown in Figure 8d involves alternating molecular (T-host) and supramolecular (O–H···O bonds) nodes. The "polar" brick-wall network of host **1** with the fluorophenol guest is a novel aggregation motif for T-shaped nodes that has so far not been observed, even among the exhaustively investigated coordination polymer and metal–ligand network solids.[8b] We define 2D polarity as the alignment of asymmetric T-shaped molecules in the same direction within a layer instead of aggregation through the centrosymmetric dimer. It is clear from the hydrogen bonding shown in Figure 8 that

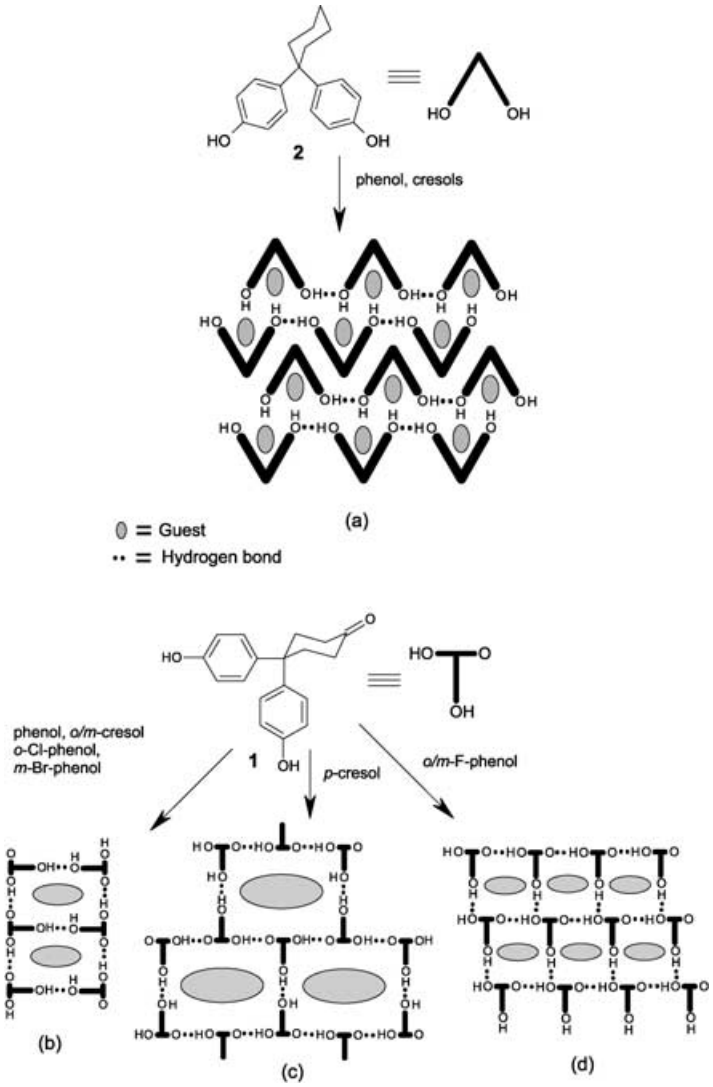

Figure 8. Host–guest self-assembly in V-shaped molecule **2** and T-shaped host **1**. There is a free phenol hydroxy in the host lattice of both **1** and **2** to bond with the guest. a) The inclusion adducts of **2** with phenol and cresols guests are isomorphous. Guest inclusion results in supramolecular isomerism of **1** to networks b), c), and d).

one phenol hydroxy group of the host is free to assist in the inclusion of OH/C=O type guests through strong hydrogen bonds, that is, that coordinato-clathration[1a] is the reason why these host molecules readily include a variety of guest/solvent molecules during crystallization. The polar brick-wall network of host **1** assembled through O–H···O bonds is topologically identical to the hexagonal network of a 2,4,6-tris(4-halophenoxy)-1,3,5-triazine host mediated by a halogen···halogen trimer synthon.[2e] The network representation is useful to relate and classify supramolecular structures of very different molecules for retrosynthetic analysis in crystal engineering.[31] The stacking arrangements of host networks of **1** are displayed in Figure 9. Phenol and aniline give chiral, ladder structures and such ladders stack through a half translation along the rungs. The larger host networks formed with the cresol guests are stacked with an offset of

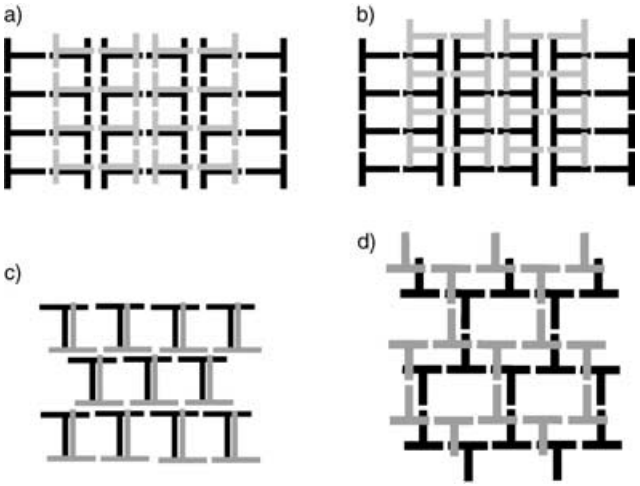

Figure 9. Stacking modes of the ladder and brick-wall networks in the inclusion complexes of host **1**. a) Stacking with an offset of half along the ladder rung in phenol and aniline clathrates. b) Stacking with an offset of half along the ladder rung and height in *o*-cresol, *m*-cresol, *o*-chlorophenol, and *m*-bromophenol adducts. c) Stacking of brick-wall layers to give rectangular channels with *o*- and *m*-fluorophenol guests. d) Stacking of brick-wall layers with an offset in the *p*-cresol adduct. Guest molecules are not shown for clarity.

half along the ladder rung and height. Polar brick-wall grids form channels for fluorophenol guest inclusion.

T-host **1** adopts two different conformations through rotation of the equatorial phenol ring in these host–guest structures. The conformation of host **1** in complexes with phenol, aniline, and *o*- and *m*-fluorophenol guests is the same because these molecules are of a similar size. Both the equatorial phenol and the axial phenol rings are roughly orthogonal to the chair cyclohexanone ring plane (see Table 3 for interplanar angles). The void size is minimal in this conformation because the equatorial phenol ring tilts into the host cavity, referred to as the "shut" windowpane conformation (Figure 10a, *o*-fluorophenol clathrate). As the guest size increases in *o*-, *m*-, and *p*-cresol, and *o*/*m*-halophenol, the host equatorial phenol ring rotates such that it is parallel to the mean plane of the cyclohexanone ring but the axial phenol remains roughly orthogonal. The cavity size is larger in this "open" windowpane conformation (Figure 10b, *o*-chlorophenol clathrate). Thus, the pore dimensions of host **1** are related to the "open" and "shut" orientations of the equatorial phenol ring (Table 3), thereby providing an interesting case of conformational and supramolecular (network) isomerism. The "shut" conformation of host **1** in Figure 10a is more stable than the "open" conformation of Figure 10b by 0.5 kcal mol^{-1} (Spartan,[32] 6-31G**), possibly because of H···H repulsion (2.0–2.1 Å) between the coplanar equatorial phenol and cyclohexanone rings in the latter conformation. Interestingly, even as the strong hydrogen-bond networks and molecular conformations change in this series of structures a recurring motif is the herringbone T-geometry (energy = 2.0–2.5 kcal mol^{-1}) of the host and guest phenol rings (Figure 10).[33] We have shown examples of supra-

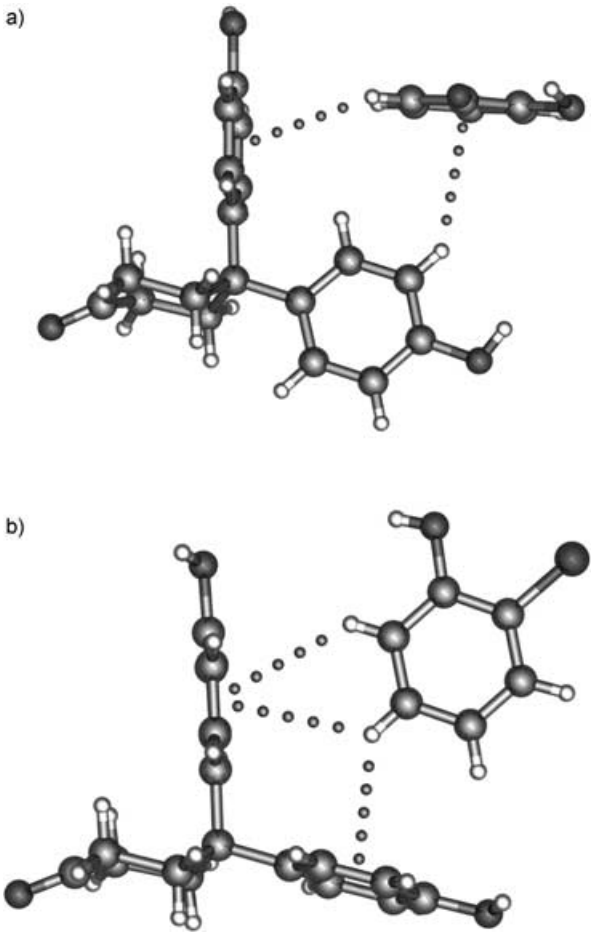

Figure 10. Conformation of the equatorial phenyl ring of T-host **1** in clathrates. The windowpane is a) "shut" in *o*-fluorophenol and b) "open" in *o*-chlorophenol as a result of rotation of the equatorial phenol by 90°, which increases the cavity size in (b). Note the herringbone T-motif between the host and guest phenyl rings, a recurring synthon in this family of host–guest structures.

molecular host–guest ladder and brick-wall assemblies constructed through strong O–H···O hydrogen bonds in which the molecular conformation and supramolecular structure are directed by guest size and aromatic interactions. Both strong O–H···O hydrogen bonds and weak phenyl–phenyl interactions imprint their distinctive signature in these host–guest structures.[34]

Lattice-energy computations: Lattice energies were calculated by minimizing the experimental X-ray structure with Cerius^2 (Dreiding2.21) force fields.[35] Despite the approximations involved in using built-in force fields, calculated crystal energies may be meaningfully compared in a family of structures because the host molecule is the same and the guest molecules have similar functional groups. Since the space group, crystal packing, and number of molecules are different for different structures, we normalize lattice energies to 1000 Å^3 of the unit cell volume. Stabilization from guest inclusion is normalized to 100 Å^3 of the guest volume. From the data in Table 4 it is evident that inclusion crystals are more stable than the guest-free form of host **1**. The role of guest size and van der Waals interactions in crystal-structure stabilization is evident from the greater contribution to the lattice energy from halophenols than from cresols, whereas phenol and aniline guests contribute the least (Figure 11). Not only guest size but intermolecular interactions too (C–H···F) play a role because the stabilization from 2- and 3-fluorophenol guests (-44.1 and -46.9 kcal mol^{-1}) is marginally greater than that from phenol (-43.9 kcal mol^{-1}).

Competition experiments and thermal analysis: One of the important applications of inclusion chemistry is the design of hosts for the separation of isomers[16] and enantiomers.[13f] Competition experiments were carried out to study the selective enclathration of phenol and aniline guests in the ladder framework of **1**. Phenol, cresols, aniline, and toluidines are constituents of coal tar among which phenol/aniline have similar sizes/shapes and boiling points (182 and 184 °C). Host **1** was crystallized from a mixture of aniline and phenol in different ratios (1:2, 1:3, 1:5, 3:1, 2:1, and 1:1) and the precipitated solid was analyzed for the included guest. In all the experiments, host **1** showed a strong preference for aniline inclusion even when phenol was present in excess. The ^{1}H NMR spectrum ([D$_6$]DMSO) of crystals of **1**·aniline obtained from a crystallization batch of 5:1 phenol/aniline showed an NH$_2$ peak for aniline at $\delta = 5.27$ ppm, but none for the hydroxy proton of phenol at $\delta = 9.60$ ppm. Thermal gravimetry of the solid sample, to confirm the host/guest ratio, was performed by directly injecting the evolved vapor through a heated transfer line into an FTIR spectrometer to analyze its vibration/rotation spectrum. Thermogravimetry-infrared (TG-IR) analysis of a **1**·aniline single

Table 4. Lattice-energy calculations on inclusion crystals of host **1** using Cerius^2 (Drieding2.21) force fields.

Guest molecule	$E_{host+guest}$ per molecule[a] [kcal mol^{-1}]	$E_{host\ only}$ per molecule[b] [kcal mol^{-1}]	$E_{guest\ only}$ per molecule[c] [kcal mol^{-1}]	V_{guest}[d] [Å^3]	$E_{host+guest}$ (1000 Å^3 of unit cell) [kcal mol^{-1}]	$E_{guest\ only}$ (100 Å^3 of guest volume) [kcal mol^{-1}]
phenol	−79.36	−44.74	−34.62	78.8	−166.34	−43.92
aniline	−78.66	−43.75	−34.90	83.7	−162.72	−41.69
o-cresol	−95.33	−32.25	−63.08	111.8	−178.57	−56.39
m-cresol	−95.28	−40.21	−55.07	112.3	−175.43	−49.04
p-cresol	−96.79	−33.02	−63.77	114.4	−181.03	−55.74
o-Cl-phenol	−124.08	−43.41	−80.67	110.8	−242.23	−72.78
m-Br-phenol	−120.07	−31.91	−88.16	118.6	−225.12	−74.34
o-F-phenol	−81.48	−45.20	−36.28	82.2	−164.41	−44.10
m-F-phenol	−86.13	−45.29	−40.84	87.0	−176.46	−46.94
guest free	−57.14	–	–	–	−160.63	–

[a] $E_{host+guest}$ = calculated lattice energy of unit cell / number of molecules in cell. This value is calibrated to 1000 Å^3 of the unit cell volume. [b] $E_{host\ only}$ = energy per molecule without solvent. [c] $E_{guest\ only}$ = stabilization from one molecule of guest. This value is calibrated to 100 Å^3 of guest volume. [d] V_{guest} = calculated volume of guest.

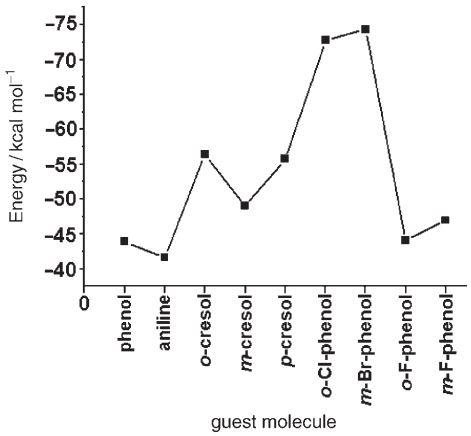

Figure 11. Contribution of guest stabilization energy (calibrated to 100 Å^3 of guest volume, Table 4) to the host–guest lattice.

crystal shows peaks for only aniline vapor in the IR spectrum (Figure 12); there is no trace of phenol. The selectivity of host **1** towards aniline over phenol, which has the same

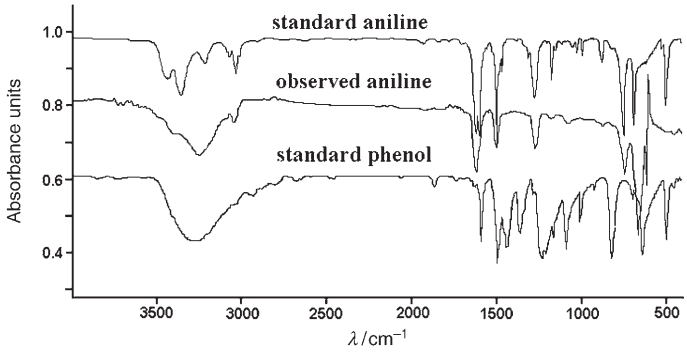

Figure 12. TG-IR spectrum of **1**·aniline shows infrared peaks for aniline vapor; there is no trace of phenol in the evolved gas. The standard spectra have been taken from the library of FTIR spectra (Bruker-Opus software). See the Supporting Information for the evolution of IR spectra with temperature.

shape/size, is due to stronger/more numerous host–guest hydrogen bonds in the former structure: each aniline molecule is bonded through three hydrogen bonds (two donors and one acceptor for each molecule) compared with 1.5 hydrogen bonds for phenol (one donor and one acceptor, one donor only). Accordingly, the energy contribution of hydrogen bonds to the crystal lattice of **1**·aniline is −51.70 kcal mol^{-1} compared with −43.85 kcal mol^{-1} for **1**·phenol (Cerius^2, Dreiding2.21). Selective inclusion of aniline and also its slower release from the host lattice relative to phenol (TGA: 140–170 °C versus 100–130 °C, Figure 13a, b) is due to the extra stabilization from 7 kcal mol^{-1} worth of hydrogen bonds in the former clathrate. Even though the hydrogen-bond energy of the aniline clathrate is substantially lower than the phenol inclusion adduct, the crystal lattice energy of the latter structure is only marginally lower (by 0.7 kcal mol^{-1}, Table 4). The agreement between computation and experiment is quite remarkable given the difficulties in accurately modeling the electrostatics of strong hydrogen-bond interactions based on the simple atomic point-charge model in Cerius^2 force fields.[11d] The fact that hydrogen-bond energy dictates the inclusion of solvent reflects the importance of kinetic factors during crystallization. Preferential enclathration of *p*-phenylenediamine from a mixture containing excess *o*-phenylenediamine (*o*/*p* 9:1) by host **2** has been ascribed to four hydrogen bonds in the former clathrate compared with two in the latter structure.[16d] However, both molecular shape and hydrogen bonding contribute towards the discrimination between *o* and *p* isomers. Selective enclathration of same size/shape guest pairs as a result of only hydrogen bonding has been illustrated by the inclusion of THF, but not cyclopentane, in a porous coordination polymer framework.[9d] Selective enclathration of phenol/aniline in a hydrogen-bonded host lattice has not been examined previously.[23]

The host/guest stoichiometries of the inclusion compounds as determined by X-ray analysis are in good agreement with the guest weight-loss measurements made by TGA (Table 5).[1e] Differences in the hydrogen-bond motifs between phenol and aniline guests in the X-ray structures are reflected in the release of these guests from the host lattice of **1** at different temperatures and rates. DSC of **1**·phenol shows a sharp endotherm at 122 °C and two molecules of phenol are lost in the temperature range of 100–130 °C in TGA. On the other hand, a major endotherm is observed at 167 °C in the DSC of **1**·aniline and guest loss occurs in the range of 140–170 °C. Release of the guests is followed by the melting of the pure host at 235 °C (Figure 13a, b). The evolution of water vapor and phenolic guests over a broad temperature range in TGA is consistent with the loss of water and cresol/halophenol guests in two endothermic steps in DSC (Figure 13c, d). The DSC and TGA thermograms are similar for adducts with similar crystal structures and hydrogen bonding, for example, *o*-cresol and *o*-chlorophenol, and *m*-cresol and *m*-bromophenol. A possible reason for phenol having a higher T_{onset} temperature than the higher boiling cresols could be that the host molecule is present in the stable ("shut") conformation found in the crystal structure of the pure host.[15] Therefore minimal reorganization of the host structure is required as the guest escapes to leave the guest-free solid. On the other hand, the release of cresol could be concomitant with a change in the host conformation from the metastable ("open") to the stable state (energy difference ~0.5 kcal mol^{-1}). Our results demonstrate that the hydrogen-bonding and host–guest packing observed in the X-ray crystal structures correlate very nicely with the selectivity of guest inclusion and the strength of host–guest interactions measured by DSC and TGA.

Conclusions

We have designed a new host molecule by deliberate functional-group modification and illustrated guest-driven self-assembly of T-shaped host **1** in ladder and brick-wall frame-

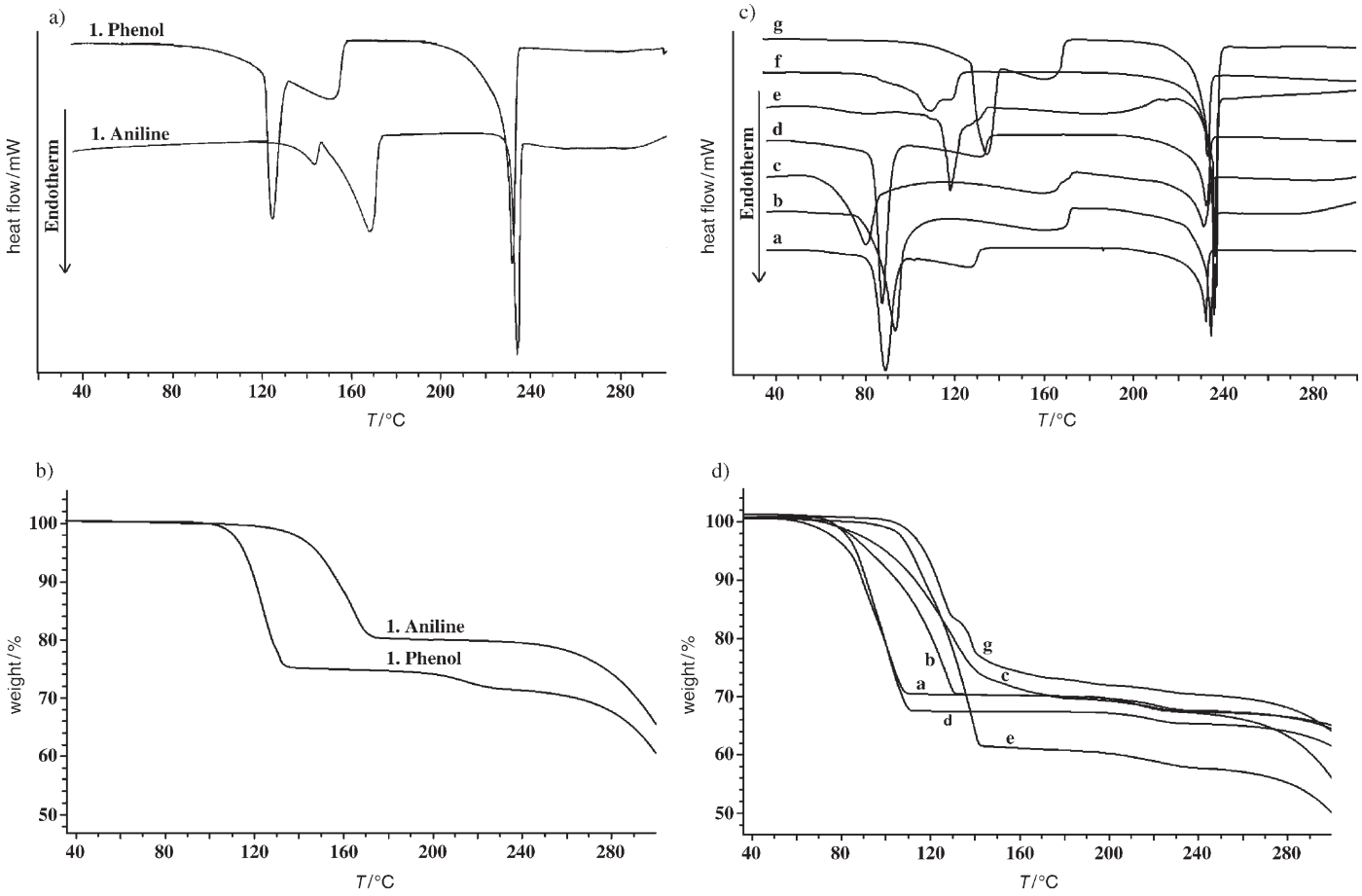

Figure 13. a) DSC and b) TGA thermograms of aniline and phenol. c) DSC and d) TGA thermograms of other guests: a = *o*-cresol, b = *m*-cresol, c = *p*-cresol, d = *o*-chlorophenol, e = *m*-bromophenol, f = *o*-fluorophenol, and g = *m*-fluorophenol. The host compound melts at 235 °C and is stable up to 300 °C. Aniline has the highest T_{onset} temperature of 140 °C in TGA and a DSC endotherm at T_{peak} = 167 °C.

works. A notable feature of host **1** is that the T-shape is built into the organic molecule and persists in both host conformations. In contrast, the T-shape of the resorcinarne-bipyidine supermolecule is found only in the flat-cone conformation of the cavitand.[7] Guest molecules control the network of **1**, from the ladder to the brick-wall structure, as a result of their different O–H···O hydrogen-bonding patterns and water molecules expand the size of rectangular pores from 80 to 280 Å^2. The conformationally flexible equatorial phenyl ring of host **1** adopts different orientations to form "open" and "shut" windowpane structures and thereby modulate the cavity size for cresol and phenol guests. Whereas strong O–H···O hydrogen bonds determine the topology of the host framework, the aromatic rings adopt a herringbone T-motif within the overall scaffold. The structure of **1** shows

Table 5. Thermal measurements (TGA and DSC) on inclusion crystals of host **1**.

Guest molecule	Calculated weight loss from X-ray structure [%]	Observed weight loss in TGA [%]	Guest loss endotherm temp. in DSC, T_{onset} [°C]	ΔH for guest loss [J g^{-1}]	Guest weight loss temperature range in TGA [°C]	Boiling point of guest [°C]
phenol	25.00	24.87	1st step: 122.4 2nd step: 132.4	191.58	111–128	182
aniline	24.80	20.96	1st step: 134.9 2nd step: 167.6	180.3	143–167	184
o-cresol	30.88	30.22	1st step: 82.3 2nd step: 118.3	156.43 42.95	80–108	191
m-cresol	30.88	30.59	1st step: 85.2 2nd step: 124.2	142.43 68.00	99–128	203
p-cresol	30.88	30.73	1st step: 67.1 2nd step: 125.0	150.75 84.29	97–143	202
o-chlorophenol	34.19	33.42	1st step: 83.4 2nd step: 107.3	141.78 39.10	83—107	175
m-bromophenol	40.38	38.89	1st step: 114.3 2nd step: 136.9	91.95 66.90	113–138	236
o-fluorophenol	28.43	–[a]	98.2	74.70	–	171
m-fluorophenol	28.43	28.27	1st step: 127.0 2nd step: 141.2	180.8	118–141	178

[a] TGA could not be performed because of sample instability.

remarkable selectivity for aniline enclathration in the presence of excess phenol (5:1) because of more numerous hydrogen bonds in the former crystal structure, providing a self-assembly approach to the separation of compounds of similar shape but with different hydrogen-bonding patterns. Crystallization from a phenol/aniline (10:1) solution yielded a rare two-in-one assembly of both guests in different regions of the molecular ladder. Thermochemical measurements have established the tenacity of host–guest interactions in this family of solids, which is related to the strength of hydrogen bonds and the stability of the host conformation in the X-ray crystal structures. Our preliminary results with fluorophenols are worthy of further investigation because these small-molecule structures are excellent models to better understand the interactions of fluorinated drugs and inhibitors with receptor proteins. The inclusion of volatile liquids and gases in a hydrophobic confinement is a current challenge in crystal engineering with immediate application in gas-storage materials. The occurrence of a three-connected polar brick-wall network, a novel aggregation mode for a T-shaped molecule, will be examined in other host–guest structures. In further studies we will focus on the introduction of electron-withdrawing/-donating groups and alkyl chains onto the phenyl rings of host **1** in order to exploit the π–π stacking and herringbone interactions[36] that modulate the host–guest architecture and to understand the effect of hydrophobic tails[37] on the resulting structures.

Experimental Section

Synthesis: A mixture of cyclohexane-1,4-dione (0.50 g, 4.5 mmol) and phenol (1.30 g, 13.9 mmol) in 1,4-dioxane (10 mL) and water (10 mL) at 0 °C was treated dropwise with conc. H_2SO_4 (6 mL). The reaction mixture was stirred at room temperature for 6 h, neutralized with $NaHCO_3$ solution, and extracted with diethyl ether to yield **1**, which was purified by column chromatography (0.69 g, 55 %).[17] ^{1}H NMR (200 MHz, [D$_6$]DMSO, 25 °C, TMS): $\delta = 8.79$ (s, 2H), 6.69 (d, $J = 8$ Hz, 4H), 6.23 (d, $J = 8$ Hz, 4H), 2.08 (t, $J = 5$ Hz, 4H), 1.81 ppm (t, $J = 5$ Hz, 4H); IR (KBr): $\tilde{\nu} = 3368$, 1696, 1611, 1512, 1440, 1371, 1236, 1181, 1013, 874, 831, 735 cm^{-1}.

Crystallization and competition experiments: Inclusion compounds were obtained by slow cooling of a saturated solution of host **1** and the corresponding guest/solvent. Single crystals appeared after a week at room temperature. Binary guest inclusion crystals were obtained from a 10:1 phenol/aniline solution.

The selectivity of guest enclathration was evaluated for aniline and phenol. Host **1** was dissolved in various molar ratios of aniline and phenol (1:5, 1:3, 1:2, 1:1, 2:1, 3:1); the resulting solution was warmed and allowed to cool slowly to ambient temperature. ^{1}H NMR spectroscopy showed inclusion of aniline but no peaks for phenol. Analysis of the gas evolved from the aniline clathrate was performed by thermogravimetry-infrared spectroscopy (TG-IR). The guest vapors evolved from the TGA instrument were passed through a coupled heated transfer line at 120 °C and characterized with a FTIR spectrometer installed with a DlaTGS detector. Sample size = 9–12 mg, heating rate = 10 °C min^{-1}, N_2 flow = 50 mL min^{-1}.

Crystal energy calculations: Dreiding2.21 force field with the charge-equilibration option was used for crystal-packing energy calculations (Cerius^2).[35] Packing coefficients for the inclusion complexes are based on free-volume calculations (Platon[38]) and the results are given in Table 4.

X-ray crystallography: X-ray data for **1**·phenol and **1**·aniline were collected at 100 K with a KUMA CCD diffractometer[39] using graphite-monochromated $Mo_{K\alpha}$ radiation. Reflections on crystals of **1**·*o*-cresol and **1**·*m*-cresol were collected with an Enraf–Nonius MACH3 diffractometer at 298 K and on crystals of **1**·*p*-cresol, **1**·*o*-chlorophenol, **1**·*o*-bromophenol, **1**·*o*-fluorophenol, **1**·*m*-fluorophenol (all at 100 K) and **1**·phenol·aniline (298 K) with a Bruker SMART APEX CCD area detector using $Mo_{K\alpha}$ radiation. Structures were solved and refined by direct methods using the SHELX[40] and SHELX-TL[41] programs. Refinement of coordinates and anisotropic thermal parameters of non-hydrogen atoms were carried out by the full-matrix least-squares refinement. All N–H and O–H protons were located in difference Fourier maps and refined isotropically. Hydrogen atoms of disordered aniline nitrogen and phenol oxygen/carbon atoms in the minor occupancy position (0.23, 0.21) were not included in the refinement. All C–H atoms were generated geometrically and allowed to ride on their parent atoms. Table 1 gives the pertinent crystallographic data for inclusion complexes of **1** and hydrogen-bond lengths are listed in Table 2.

CCDC-268053–CCDC-268062 contains the supplementary crystallographic data for this paper. These data can be obtained free of charge from the Cambridge Crystallographic Data Center via www.ccdc.cam.ac.uk/data_request/cif.

Thermal analysis: Differential scanning calorimetry (DSC) was performed with a Mettler Toledo DSC 822e module and thermogravimetry (TGA) was performed with a Mettler Toledo TGA/SDTA 851e module. Crystals taken from the mother liquor were blotted dry on filter paper and placed in open alumina pans for the TG experiments and in crimped but vented aluminium sample pans for the DSC experiments. The sample size for DSC was 4–6 mg and for TGA was 8–12 mg. The temperature range was typically 30–300 °C at a heating rate of 10 °C min^{-1}. The samples were purged with a stream of nitrogen flowing at 150 mL min^{-1} for DSC and 50 mL min^{-1} for TG measurements. The TG instrument was coupled to a Bruker Tensor FT-IR spectrometer via a heated transfer line for EGA (evolved gas analysis).

Acknowledgements

A.N. thanks the DST for funding (SR/S5/OC-02/2002) and S.A. thanks the CSIR for a fellowship. The DST (IRPHA) provided funds for the CCD diffractometer and the UPE program is supported by the UGC. We thank Prof. M. Jaskólski (University of Adam Mickiewicz, Poland) and L. S. Reddy (University of Hyderabad) for assistance with X-ray data collection.

[1] a) D. D. MacNicol, F. Toda, R. Bishop (Eds.), *Comprehensive Supramolecular Chemistry, Vol. 6*: *Solid-State Supramolecular Chemistry, Crystal Engineering*, Pergamon Press, Oxford, **1996**; b) R. Bishop, *Synlett* **1999**, *9*, 1351; c) A. Nangia, *Curr. Opin. Solid State Mater. Sci.* **2001**, *6*, 115; d) K. T. Holman, A. M. Pivovar, J. A. Swift, M. D. Ward, *Acc. Chem. Res.* **2001**, *34*, 107; e) L. R. Nassimbeni, *Acc. Chem. Res.* **2003**, *36*, 631; f) M. R. Caira in *Encyclopedia of Supramolecular Chemistry, Vol. 1* (Eds.: J. L. Atwood, J. W. Steed), Marcel Dekker, New York, **2004**, pp. 767–775; g) A. Nangia in *Nanoporous Materials: Science and Engineering* (Eds.: G. Q. Lu, X. S. Zhao), Imperial College Press, London, **2004**, pp. 165–187; h) E. E. Nifantyev, V. I. Maslennikova, R. V. Merkulov, *Acc. Chem. Res.* **2005**, *38*, 108.

[2] a) C. V. K. Sharma, A. Clearfield, *J. Am. Chem. Soc.* **2000**, *122*, 4394; b) D. J. Plaut, K. M. Lund, M. D. Ward, *Chem. Commun.* **2000**, 769; c) M. J. Zaworotko, *Chem. Commun.* **2001**, 1; d) B.-Q. Ma, P. Coppens, *Chem. Commun.* **2003**, 2290; e) B. K. Saha, R. K. R. Jetti, L. S. Reddy, S. Aitipamula, A. Nangia, *Cryst. Growth Des.* **2005**, *5*, 887.

[3] a) R. Thaimattam, R. Xue, J. A. R. P. Sarma, T. C. W. Mak, G. R. Desiraju, *J. Am. Chem. Soc.* **2001**, *123*, 4432; b) J. H. Fournier, T.

Maris, J. D. Wuest, W. Z. Guo, E. Galoppini, *J. Am. Chem. Soc.* **2003**, *125*, 1002; c) J. -H. Fournier, T. Maris, J. D. Wuest, *J. Org. Chem.* **2004**, *69*, 1762; d) B. R. Bhogala, P. Vishweshwar, A. Nangia, *Cryst. Growth Des.* **2005**, 5, 1271.

[4] For examples of organic ladders from T-shaped molecules, see: a) S. Aitipamula, P. K. Thallapally, R. Thaimattam, M. Jaskólski, G. R. Desiraju, *Org. Lett.* **2002**, *4*, 921; b) V. S. S. Kumar, F. C. Pigge, N. P. Rath, *New J. Chem.* **2003**, *27*, 1554.

[5] For examples of hydrogen-bonded ladders from molecules not having a T-shape, see: a) V. T. Nguyen, P. D. Ahn, R. Bishop, M. L. Scudder, D. C. Craig, *Eur. J. Org. Chem.* **2001**, 4489; b) C. Glidewell, J. N. Low, J. M. S. Skalke, J. L. Wardell, *Acta Crystallogr., Sect. C* **2002**, *58*, o201; c) M.-K. Leung, A. B. Bandal, C.-C. Wang, G.-H. Lee, S.-M. Peng, H.-L. Cheng, G.-R. Her, I. Chao, H.-F. Lu, Y.-C. Sun, M.-Y. Shiao, P.-T. Chou, *J. Am. Chem. Soc.* **2002**, *124*, 4287; d) A. D. Bond, *Chem. Eur. J.* **2004**, *10*, 1885; molecular ladders or [*n*]-ladderanes: e) H. Höpf, *Angew. Chem.* **2004**, *116*, 2928; *Angew. Chem. Int. Ed.* **2003**, *42*, 2822; f) X. Gao, T. Friščic, L. R. MacGillivray, *Angew. Chem.* **2003**, *115*, 234; *Angew. Chem. Int. Ed.* **2004**, *43*, 232.

[6] For examples of brick-wall networks from T-shaped organic molecules, see: a) P. Vishweshwar, A. Nangia, V. M. Lynch, *J. Org. Chem.* **2002**, *67*, 556; b) V. S. S. Kumar, A. Nangia, M. T. Kirchner, R. Boese, *New J. Chem.* **2003**, *27*, 224.

[7] For examples of brick-wall networks from T-shaped organic supermolecules, see: a) Y. Zhang, C. D. Kim, P. Coppens, *Chem. Commun.* **2000**, 2299; b) L. R. MacGillivray, K. T. Holman, J. L. Atwood, *J. Supramol. Chem.* **2001**, *1*, 125; c) L. R. MacGillivray, J. L. Reid, J. A. Ripmeester, *Chem. Commun.* **2001**, 1034; d) B.-Q. Ma, P. Coppens, *Chem. Commun.* **2003**, 412; e) B.-Q. Ma, P. Coppens, *Chem. Commun.* **2003**, 504.

[8] a) G. R. Desiraju, *Angew. Chem.* **1995**, *107*, 2541; *Angew. Chem. Int. Ed. Engl.* **1995**, *34*, 2311; b) B. Moulton, M. J. Zaworotko, *Chem. Rev.* **2001**, *101*, 1629; c) A. Nangia, *CrystEngComm* **2002**, *4*, 93; d) G. R. Desiraju, *J. Mol. Struct.* **2003**, *656*, 5; e) D. Braga, L. Brammer, N. R. Champness, *CrystEngComm* **2005**, *7*, 1.

[9] a) R. K. R. Jetti, F. Xue, T. C. W. Mak, A. Nangia, *J. Chem. Soc., Perkin Trans. 2* **2000**, 1223; b) K. T. Holman, S. M. Martin, D. P. Parker, M. D. Ward, *J. Am. Chem. Soc.* **2001**, *123*, 4421; c) E. Weber, S. Nitsche, A. Wierig, I. Csöregh, *Eur. J. Org. Chem.* **2002**, 856; d) K. Uemura, S. Kitagawa, M. Kondo, K. Fukui, R. Kitaura, H.-C. Chang, T. Mizutani, *Chem. Eur. J.* **2002**, *8*, 3587; e) K. Kobayashi, A. Sato, S. Sakamoto, K. Yamaguchi, *J. Am. Chem. Soc.* **2003**, *125*, 3035; f) R. Matsufa, R. Kitaura, S. Kitagawa, Y. Kubota, T. C. Kobayashi, S. Horike, M. Takata, *J. Am. Chem. Soc.* **2004**, *126*, 14063; g) C. M. Reddy, L. S. Reddy, S. Aitipamula, A. Nangia, C.-K. Lam, T. C. W. Mak, *CrystEngComm* **2005**, *7*, 44.

[10] a) A. T. Ung, R. Bishop, D. C. Craig, I. G. Dance, M. L. Scudder, *Tetrahedron* **1993**, *49*, 639; b) K. Nakano, K. Sada, M. Miyata, *Chem. Commun.* **1996**, 989; c) K. Nakano, M. Katsuta, K. Sada, M. Miyata, *CrystEngComm* **2001**, *11*, 1.

[11] a) G. R. Desiraju, *Nat. Mater.* **2002**, *1*, 77; b) J. D. Dunitz, *Chem. Commun.* **2003**, 545; c) W. D. S. Motherwell, H. L. Ammon, J. D. Dunitz, A. Dzyabchenko, P. Erk, A. Gavezzotti, D. W. M. Hofmann, F. J. J. Leusen, J. P. M. Lommerse, W. T. M. Mooij, S. L. Price, H. Scheraga, B. Schweizer, M. U. Schmidt, B. P. van Eijck, P. Verwer, D. E. Williams, *Acta Crystallogr. Sect. B* **2002**, *58*, 647; d) G. M. Day, J. Chisholm, N. Shan, W. D. S. Motherwell, W. Jones, *Cryst. Growth Des.* **2004**, *4*, 1327.

[12] For some recent reviews on metal–organic frameworks and hybrid structures, see: a) M. Eddaoudi, B. B. Moler, H. Li, B. Chen, T. M. Reineke, M. O'Keeffe, O. M. Yaghi, *Acc. Chem. Res.* **2001**, *34*, 319; b) O. R. Evans, W. Lin, *Acc. Chem. Res.* **2002**, *35*, 511; c) S. L. James, *Chem. Soc. Rev.* **2003**, *32*, 276; d) K. Biradha, *CrystEngComm* **2003**, *5*, 374; e) S. A. Barnett, N. R. Champness, *Coord. Chem. Rev.* **2003**, *246*, 145; f) S. Kitagawa, R. Kitaura, S. Noro, *Angew. Chem.* **2004**, *116*, 2388; *Angew. Chem. Int. Ed.* **2004**, *43*, 2334; g) N. W. Ockwig, O. Delgado-Friedrichs, M. O'Keeffe, O. M. Yaghi, *Acc. Chem. Res.* **2005**, *38*, 176; h) S. Kitagawa, K. Uemura, *Chem. Soc. Rev.* **2005**, *34*, 109.

[13] a) J. L. Atwood, L. J. Barbour, A. Jerga, *Science* **2002**, *296*, 2367; b) J. L. Atwood, L. J. Barbour, A. Jerga, B. L. Schottel, *Science* **2002**, *298*, 1000; c) J. L. Atwood, L. J. Barbour, A. Jerga, *Angew. Chem.* **2004**, *116*, 3008; *Angew. Chem. Int. Ed.* **2004**, *43*, 2948; d) J. L. Atwood, L. J. Barbour, P. K. Thallapally, T. B. Wirsig, *Chem. Commun.* **2005**, 51; e) P. Sozzani, S. Bracco, A. Comotti, R. Simonutti, *Angew. Chem.* **2005**, *117*, 1850; *Angew. Chem. Int. Ed.* **2005**, *44*, 1816; f) J. L. Atwood, S. J. Dalgarno, M. J. Hardie, C. L. Raston, *Chem. Commun.* **2005**, 337.

[14] S. Aitipamula, A. Nangia, *Supramol. Chem.* **2005**, *17*, 17.

[15] S. Aitipamula, G. R. Desiraju, M. Jaskólski, A. Nangia, R. Thaimattam, *CrystEngComm* **2003**, *5*, 447.

[16] a) I. Goldberg, Z. Stein, A. Kai, F. Toda, *Chem. Lett.* **1987**, 1617; b) I. Goldberg, Z. Stein, K. Tanaka, F. Toda, *J. Inclusion Phenom.* **1988**, *6*, 15; c) F. Toda, K. Tanaka, T. Fujiwara, *Angew. Chem.* **1990**, *102*, 688; *Angew. Chem. Int. Ed. Engl.* **1990**, *29*, 662; d) M. R. Caira, A. Horne, L. R. Nassimbeni, K. Okuda, F. Toda, *J. Chem. Soc., Perkin Trans.* 2 **1995**, 1063; e) M. R. Caira, A. Horne, L. R. Nassimbeni, F. Toda, *J. Mater. Chem.* **1997**, *7*, 2145; f) M. R. Caira, A. Horne, L. R. Nassimbeni, F. Toda, *J. Chem. Soc., Perkin Trans. 2* **1997**, 1717; g) M. R. Caira, A. Horne, L. R. Nassimbeni, F. Toda, *J. Mater. Chem.* **1998**, *8*, 1481; h) Z. Urbanczyk-Lipkowska, K. Yoshizawa, S. Toyota, F. Toda, *CrystEngComm* **2003**, *5*, 144.

[17] T. Kolasa, D. E. Gunn, P. Bhatia, A. Basha, R. A. Craig, A. O. Stewart, J. B. Bouska, R. R. Harris, K. I. Hulkower, P. E. Malo, R. L. Bell, G. W. Carter, C. D. Brooks, *J. Med. Chem.* **2000**, *43*, 3322.

[18] O. Ermer, A. Eling, *J. Chem. Soc., Perkin Trans. 2* **1994**, 925.

[19] a) A. Anthony, M. Jaskólski, A. Nangia, G. R. Desiraju, *Chem. Commun.* **1998**, 2537; b) A. Anthony, M. Jaskólski, A. Nangia, *Acta Crystallogr. Sect. B* **2000**, *58*, 512.

[20] a) S. Apel, S. Nitsche, K. Beketov, W. Seichter, J. Seidel, E. Weber, *J. Chem. Soc., Perkin Trans. 2* **2001**, 1212; b) L. J. Barbour, M. R. Caira, T. Le Roex, L. R. Nassimbeni, *J. Chem. Soc., Perkin Trans. 2* **2002**, 1973; c) J. L. Atwood, A. Szumna, *Chem. Commun.* **2003**, 940.

[21] a) H. Koshima, K. Ding, Y. Chisaka, T. Matsuura, *J. Am. Chem. Soc.* **1996**, *118*, 12059; b) T. B. Norstein, R. McDonald, N. R. Branda, *Chem. Commun.* **1999**, 719; c) M. P. Lightfoot, F. S. Mair, R. G. Pritchard, J. E. Warren, *Chem. Commun.* **1999**, 1945; d) K. Tanaka, D. Fujimoto, T. Oeser, H. Irngartinger, F. Toda, *Chem. Commun.* **2000**, 413; e) R. K. R. Jetti, A. Nangia, F. Xue, T. C. W. Mak, *Chem. Commun.* **2001**, 919; f) L. P. García, D. B. Amabilino, *Chem. Soc. Rev.* **2002**, *31*, 342; g) E. Pidcock, *Chem. Commun.* **2005**, 3457.

[22] C. P. Brock, L. L. Duncan, *Chem. Mater.* **1994**, *6*, 1307.

[23] a) M. Shibakami, A. Sekiya, *J. Chem. Soc., Chem. Commun.* **1994**, 429; b) K. Nakano, K. Sada, Y. Kurozumi, M. Miyata, *Chem. Eur. J.* **2001**, *7*, 209.

[24] G. A. Jeffrey, *An Introduction to Hydrogen Bonding*, Oxford University Press, New York, **1997**, pp. 98–116.

[25] a) R. K. R. Jetti, P. K. Thallapally, F. Xue, T. C. W. Mak, A. Nangia, *Tetrahedron* **2000**, *56*, 6707; b) S. George, A. Nangia, M. Bagieu-Beucher, R. Masse, J.-F. Nicoud, *New J. Chem.* **2003**, *27*, 568; c) A. I. Kitaigorodsky, *Molecular Crystals and Molecules*, Academic Press, New York, **1973**, p. 20.

[26] a) N. N. L. Madhavi, A. K. Katz, H. L. Carrell, A. Nangia, G. R. Desiraju, *Chem. Commun.* **1997**, 1953; b) M. Nishio, *CrystEngComm* **2004**, *6*, 130.

[27] A. R. Choudhury, T. N. G. Row, *Cryst. Growth Des.* **2004**, *4*, 47.

[28] a) M. Shibakami, A. Sekiya, *J. Chem. Soc., Chem. Commun.* **1992**, 1742; b) G. D. Enright, K. A. Udachin, J. A. Ripmeester, *Chem. Commun.* **2004**, 1360.

[29] J. D. Dunitz, R. Taylor, *Chem. Eur. J.* **1997**, *3*, 89.

[30] a) D. O'Hagan, H. S. Rzepa, *Chem. Commun.* **1997**, 645; b) E. A. Meyer, R. K. Castellano, F. Diederich, *Angew. Chem.* **2003**, *115*, 1244; *Angew. Chem. Int. Ed.* **2003**, *42*, 1210; c) F. Hof, F. Diederich, *Chem. Commun.* **2004**, 477.

[31] L. S. Reddy, B. R. Bhogala, A. Nangia, *CrystEngComm* **2005**, *7*, 206.

[32] www.wavefun.com
[33] The herringbone geometry between host and guest phenyl rings is reminiscent of the crystal structure of pure benzene and naphthalene. Similar observations have been noted in the guanadinium sulfonate (GS) host (see ref. [1d]) and coordination polymer structures with aromatic guests. a) K. Biradha, D. Dennis, V. A. MacKinnon, C. V. K. Sharma, M. J. Zaworotko, *J. Am. Chem. Soc.* **1998**, *120*, 11894; b) K. Biradha, K. V. Domasevitch, B. Moulton, S. Seward, M. J. Zaworotko, *Chem. Commun.* **1999**, 1327.
[34] For some recent examples of host–guest structures that involve aromatic···aromatic interactions, see: a) J. L. Atwood, L. J. Barbour, C. L. Raston, I. B. N. Sudria, *Angew. Chem.* **1998**, *110*, 1029; *Angew. Chem. Int. Ed.* **1998**, *37*, 981; b) M. R. Caira, L. R. Nassimbeni, F. Toda, D. Vujovic, *J. Chem. Soc., Perkin Trans.* 2, **1999**, 2681; c) M. R. Caira, L. R. Nassimbeni, F. Toda, D. Vujovic, *J. Am. Chem. Soc.* **2000**, *122*, 9367; d) S. R. Alshahateet, R. Bishop, D. C. Craig, M. C. Scudder, *CrystEngComm* **2001**, *3*, 225; e) R. Bishop, A. N. M. M. Rahman, J. Ashmore, D. C. Craig, M. C. Scudder, *CrystEngComm* **2002**, *4*, 605; f) L. R. Nassimbeni, H. Su, E. Weber, K. Skobridis, *Cryst. Growth Des.* **2004**, *4*, 85.
[35] www.accelrys.com
[36] a) C. Janiak, *J. Chem. Soc., Dalton Trans.* **2000**, 3885; b) W. B. Jennings, B. M. Farrell, J. F. Malone, *Acc. Chem. Res.* **2001**, *34*, 885; c) V. R. Vangala, A. Nangia, V. M. Lynch, *Chem. Commun.* **2002**, 51; d) L. S. Reddy, A. Nangia, V. M. Lynch, *Cryst. Growth Des.* **2004**, *4*, 89.
[37] G. W. V. Cave, J. Antesberger, L. J. Barbour, R. M. McKinlay, J. L. Atwood, *Angew. Chem.* **2004**, *116*, 5375; *Angew. Chem. Int. Ed.* **2004**, *43*, 5263.
[38] A. L. Spek, PLATON: A Multipurpose Crystallographic Tool, Utrecht University, The Netherlands, **1998**.
[39] KUMA: KM-4 Software and CrysAlis, Kuma Diffraction, Wroclaw, Poland, **1999**.
[40] G. M. Sheldrick, SHELXS-97 and SHELXL-97, Program for the Solution and Refinement of Crystal Structures, University of Göttingen (Germany), **1997**.
[41] SHELX-TL (version 6.14), Program for the Solution and Refinement of Crystal Structures, Bruker AXS, Wisconsin (USA), **2000**.

Received: April 8, 2005
Published online: August 30, 2005

